Inorganica Chimica Acta 499 (2020) 119178

Contents lists available at ScienceDirect

Inorganica Chimica Acta

journal homepage: www.elsevier.com/locate/ica

Research paper

Three- and two-site heteropolyoxotungstate anions as catalysts for the epoxidation of allylic alcohols by H_2O_2 under biphasic conditions: Reactivity and kinetic studies of the $[Ni_3(OH_2)_3(B\text{-}PW_9O_{34})\{WO_5(H_2O)\}]^{7-}$, $[Co_3(OH_2)_6(A\text{-}PW_9O_{34})_2]^{12-}$, and $[M_4(OH_2)_2(B\text{-}PW_9O_{34})_2]^{10-}$ anions, where M = Mn(II), Co(II), Ni(II), Cu(II) and Zn(II)

Paulus Hengky Abram[a,b], Robert C. Burns[a,*], Lichun Li[a,1]

[a] Discipline of Chemistry, School of Environmental and Life Sciences, The University of Newcastle, Callaghan, New South Wales 2308, Australia
[b] Department of Chemistry, Faculty of Education, University of Tadulako, Jl. Sukarno Hata Km. 9, Palu, Indonesia

ARTICLE INFO

Keywords:
$[Ni_3(OH_2)_3(B\text{-}PW_9O_{34})\{WO_5(H_2O)\}]^{7-}$
$[Co_3(OH_2)_6(A\text{-}PW_9O_{34})_2]^{12-}$
$[M^{II}_4(OH_2)_2(B\text{-}PW_9O_{34})_2]^{10-}$ (M^{II} = Mn, Co, Ni, Cu, Zn)
Epoxidation
Allylic alcohols
Autocatalysis

ABSTRACT

The trimetallic phosphopolyoxotungstate anions $[Ni_3(OH_2)_3(B\text{-}PW_9O_{34})\{WO_5(H_2O)\}]^{7-}$ and $[Co_3(OH_2)_6(A\text{-}PW_9O_{34})_2]^{12-}$ have been studied as epoxidation catalysts for oxygen transfer from 30% H_2O_2 to a range of allylic alcohols under biphasic conditions (1,2-dichloroethane/H_2O) at 15 °C. The reaction mechanism involves co-ordination of an allylic alcohol at an M(II) site in each case, prior to transfer of a peroxy oxygen from an adjacent $W(O_2)$ site. The latter is formed from a terminal W = O unit by reaction with H_2O_2. Evidence of $W(O_2)$ formation was obtained through IR studies. The $W(O_2)$ group forms the epoxide by transfer of an oxygen atom to the C═C bond of the coordinated allylic alcohol. Kinetic studies using 3-methyl-2-buten-1-ol as the allylic alcohol substrate have been modelled with all three metal sites catalytically active. The reaction involves an autocatalysis mechanism involving an induction period, which can be rationalised by proposing not only coordination of the allylic alcohol to M(II), but also the product hydroxy epoxide, both through their –OH groups. The autocatalysis is generated by formation of the $W(O_2)$ group adjacent to a coordinated hydroxy epoxide, which competes with coordination of allylic alcohol. The mechanism requires some twenty-one steps involving just the generic steps listed above, with all three metal sites catalytically active. Temperature-dependent kinetic studies and subsequent Eyring analyses have shown that the Co(II)-containing catalyst is the most active of the two. Analogous studies of the epoxidation of 3-methyl-2-buten-1-ol by the two-site $[M_4(OH_2)_2(B\text{-}PW_9O_{34})_2]^{10-}$ ions as catalysts, where M = Mn(II), Co(II), Ni(II), Cu(II) and Zn(II), at 15 °C gave an order of reactivity of Cu(II) > Ni(II) > Zn (II), Co(II), Mn(II), which mostly mimics the natural order of stability constants (the Irving-Williams series), suggesting that the formation of the allylic alcohol complexes play a dominant role in this series of related complex anions, with greater replacement of water by allylic alcohol leading to greater reactivity.

1. Introduction

Oxidation of organic substrates such as alkanes, alkenes, as well as both primary and secondary alcohols has been studied extensively using both isopoly- and heteropoly-oxometalates as catalysts under homogeneous and biphasic reaction conditions with a variety of oxidants. These oxidants include species such as molecular oxygen, H_2O_2, iodosylarenes, alkyl peroxides, *t*-butyl hydroperoxide, periodate, peroxomonosulfate (HSO_5^-), etc. [1–5]. Of all these oxidants, other than O_2 itself, H_2O_2 is the best as it provides 47% active oxygen while the reduction product is the environmentally friendly H_2O [5]. However, both O_2 and H_2O_2 generally demonstrate complex oxidation chemistry with little control over the reactions. A comprehensive review of earlier work using the above oxidants with transition metal-substituted polyoxometalates has been given by Hill and co-workers [1,5]. Most reactions that involved O_2 as the oxidant examined alkanes and alkenes and were carried out at higher temperatures (room temperature to 150 °C), and generally resulted in several reaction products. Reactions that

---

* Corresponding author.
E-mail addresses: Robert.Burns@newcastle.edu.au (R.C. Burns), lichunli@zjut.edu.cn (L. Li).
[1] Present address: College of Chemical Engineering, Zhejiang University of Technology, 18 Chaowang Road, Hangzhou 310014, PR China.

https://doi.org/10.1016/j.ica.2019.119178
Received 12 July 2019; Received in revised form 27 September 2019; Accepted 27 September 2019
Available online 28 September 2019

involved aqueous H_2O_2 were performed at about room temperature, but also generated multiple products. Several structural types of heteropolyoxometalates are considered to be robust, oxidation-resistant inorganic metalloporphyrin analogues under the conditions employed for these reactions [1–5].

The most successful heteropolyoxometalate catalysts are the sandwich-type species, such as the $[WZn\{M(OH_2)\}_2(B\text{-}ZnW_9O_{34})_2]^{m-}$ ions, where M = Mn(II), Co(II), Ni(II), Cu(II), Zn(II), Pd(II) and Pt(II), with m = 12; Fe(III) and Rh(III), with m = 10 and Ru(III), with m = 11 (there is a coordinated OH^- in place of an H_2O molecule in this anion) [6–8]. These species have been used to epoxidise alkenes and/or primary and secondary allylic alcohols under biphasic conditions using aqueous H_2O_2 at about room temperature [7–14]. Other heteropolyoxotungstate anions that have functioned as successful catalysts for the epoxidation of alkenes or allylic alcohols using H_2O_2 under biphasic conditions include the mono-substituted Dawson ions $[\alpha_2\text{-}P_2W_{17}O_{61}M(L)]^{n-}$, where M = Co(II), Ni(II), Zn(II), Pd(II), Cr(III), Mn(III), Fe(III) and Ir(IV) (with L = Br^- or H_2O) [15], and also the Ni(II)-substituted quasi-Dawson-type fluoro-oxotungstate $[Ni(OH_2)H_2F_6NaW_{17}O_{55}]^{9-}$ [16]. Related sandwich-type species that have been studied for alkene oxidation include the $[(Fe^{III})_4(OH_2)_2(B\text{-}PW_9O_{34})_2]^{6-}$ and $[(Fe^{III})_4(OH_2)_2(P_2W_{15}O_{56})_2]^{12-}$ ions [17,18], the $[(Fe^{II})_4(B\text{-}PW_9O_{34})_2]^{10-}$ ion [19], and the three Mn(II)-containing $[\{Mn^{II}(OH_2)_3\}_2(WO_2)_2(BiW_9O_{33})_2]^{10-}$, $[\{Mn^{II}(OH_2)_3\}_2(SbW_9O_{33})_2]^{12-}$ and $[\{Mn^{II}(OH_2)_3\}_2\{Mn^{II}(OH_2)_2\}_2(TeW_9O_{33})_2]^{18-}$ ions [20]. For allylic alcohols, epoxidation is highly important as epoxides may be used as raw materials for epoxy resins as well as for the synthesis of biologically important molecules, as epoxidation leads to the formation of chiral centers [21–24].

Transition metal sandwich compounds have also been used for other oxidations. The spontaneous assembly of $[WZn\{Zn(OH_2)\}_2(B\text{-}ZnW_9O_{34})_2]^{12-}$ from Na_2WO_4 and $Zn(NO_3)_2$ has been reported, where it was used for the *in situ* oxidation of ammonia with H_2O_2 to hydroxylamine, which in turn reacted with ketones and aldehydes to yield oximes [25]. Other organic reactions catalysed by heteropolyoxometalates have been reviewed by Qiao and Hou [26], and even the oxidative desulfurization of fuel oils can be accomplished by heteropolyoxometalates among other environmental applications [27,28].

Recently, we have studied the comparative catalytic activities of the transition metal-substituted $[WZn\{M(OH_2)\}_2(B\text{-}ZnW_9O_{34})_2]^{12-}$ sandwich anions, where M = Mn(II), Co(II), Ni(II), Cu(II) and Zn(II), for the epoxidation of a selected series of allylic alcohols and related species using aqueous H_2O_2 as the source of oxygen under biphasic conditions [14]. For these studies we chose aqueous H_2O_2 as the oxidant based on our previous studies using transition metal-substituted Dawson anions as catalysts as the reactions were controllable and resulted in few side products [15]. Molecular oxygen was unreactive under the chosen experimental conditions. The reactions were performed under experimental conditions whereby the substituted metal ions, M(II), in the waist of the anions were able to demonstrate their role in the epoxidation reaction and established the order for these labile first row transition metal ions of Zn(II) > Mn(II) ~ Cu(II) > Co(II) > Ni(II). This order was related to the rate of exchange of the aqua groups on the substituted M(II) ions, and implied the coordination of the allylic alcohol at an M(II) site as part of the reaction mechanism. Other steps included formation of a $W(O_2)$ site adjacent to the coordinated allylic alcohol and subsequent peroxo oxygen transfer to the coordinated allylic alcohol. A kinetic study of the epoxidation of a selected allylic alcohol, 3-methy-2-buten-1-ol, by aqueous H_2O_2 was also studied under biphasic conditions using the $[WZn\{Mn(OH_2)\}_2(B\text{-}ZnW_9O_{34})_2]^{12-}$ ion as the catalyst. This study showed that the epoxidation followed an autocatalysis mechanism, which involved not only coordination of the allylic alcohol, but also the product hydroxy epoxide to M(II), both through their –OH groups. The $[WZn\{Mn(OH_2)\}_2(B\text{-}ZnW_9O_{34})_2]^{12-}$ ion has two Mn(II) sites where coordination of allylic alcohol can occur, but there are examples of transition metal-substituted heteropolyoxotungstate anions that have three M(II) sites, such as the $[Ni_3(OH_2)_3(B\text{-}PW_9O_{34})\{WO_5(H_2O)\}]^{7-}$ and $[Co_3(OH_2)_6(A\text{-}PW_9O_{34})_2]^{12-}$ ions (note that the latter is a reformulation of the anion in the compound originally described by Knoth et al. as $K_{12}[Co_3(OH_2)_3(A\text{-}PW_9O_{34})_2].10H_2O$; see also below for further description of this structure) [29–31]. Representations of these two anions are shown in Figs. 1 and 2, respectively. The increase in the number of sites may provide more active anions for epoxidation reactions of allylic alcohols under biphasic conditions. Other examples of interest are the related two-site $[M_4(OH_2)_2(B\text{-}PW_9O_{34})_2]^{10-}$ ions, where M = Mn(II), Co(II), Ni(II), Cu(II) and Zn(II) [30,32–35]. A representation of a two-site $[M_4(OH_2)_2(B\text{-}PW_9O_{34})_2]^{10-}$ ion is shown in Fig. 3. In these anions the heteropolyoxotungstate "sandwich" component $[B\text{-}ZnW_9O_{34}]^{12-}$ has been replaced by a $[B\text{-}PW_9O_{34}]^{9-}$ ion, lowering the overall charge of the entire catalyst anion (i.e. from −12 to −10), as well as introducing structural changes because of the change from Zn(II) to P(V). None of these two- or three-site anions have been used previously as oxygen transfer catalysts for the epoxidation of alkenes or allylic alcohols by H_2O_2 under biphasic conditions.

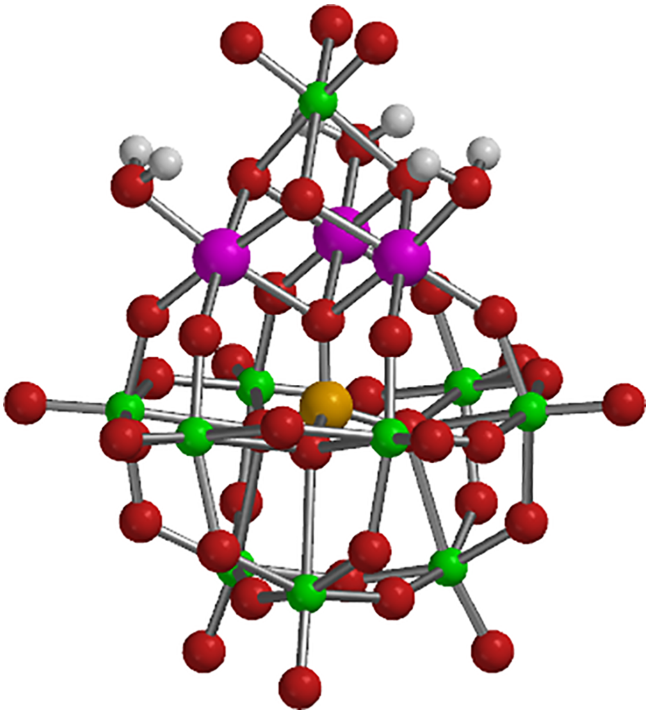

Fig. 1. A representation of the $[Ni_3(OH_2)_3(B\text{-}PW_9O_{34})\{WO_5(H_2O)\}]^{7-}$ anion. Colours: pink, Ni; green, W; orange, P; red, O; white, H. Note that the two H atoms of the H_2O in the $\{WO_5(H_2O)\}$ unit are not included in the diagram and are assumed to be disordered around the three terminal O atoms. (For interpretation of the references to colour in this figure legend, the reader is referred to the web version of this article.)

The present studies examine the relative catalytic activities of the three-site $[Ni_3(OH_2)_3(B\text{-}PW_9O_{34})\{WO_5(H_2O)\}]^{7-}$ and $[Co_3(OH_2)_6(A\text{-}PW_9O_{34})_2]^{12-}$ ions and compares them with that of the previously studied two-site $[WZn\{Mn(OH_2)\}_2(B\text{-}ZnW_9O_{34})_2]^{12-}$ ion in a series of epoxidations of selected primary allylic alcohols and related compounds using aqueous H_2O_2 as the oxidant, as well as kinetic studies of these three-site anions in the epoxidation of 3-methyl-2-buten-1-ol by H_2O_2 under biphasic conditions, i.e. 1,2-dichloroethane (1,2-dce)/aqueous H_2O_2. Studies are also reported on the $[M_4(OH_2)_2(B\text{-}PW_9O_{34})_2]^{10-}$ series of ions, where M = Mn(II), Co(II), Ni(II), Cu(II) and Zn(II), as epoxidation catalysts for allylic alcohols under identical reaction conditions.

2. Experimental

2.1. General

2.1.1. Materials and equipment

All materials used were of analytical or reagent grade and were

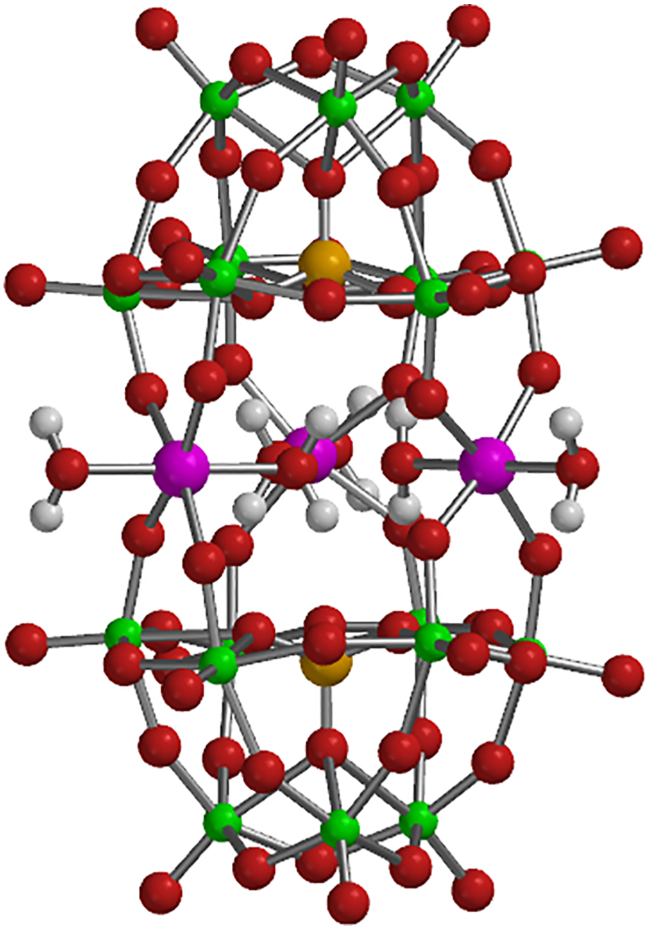

Fig. 2. A representation of the $[Co_3(OH_2)_6(B\text{-}PW_9O_{34})_2]^{12-}$ anion. Colours: pink, Co; green, W; orange, P; red, O; white, H. (For interpretation of the references to colour in this figure legend, the reader is referred to the web version of this article.)

obtained commercially, as indicated below. All were used without further purification. The following materials were employed in the synthesis of the compounds: $Na_2WO_4\cdot 2H_2O$ (99%, Sigma-Aldrich), $Zn(NO_3)_2\cdot 6H_2O$ (98%, Sigma-Aldrich), $Mn(NO_3)_2\cdot 6H_2O$ (98%, APS), $Co(NO_3)_2\cdot 6H_2O$ (98–102%, Univar), $Ni(NO_3)_2\cdot 6H_2O$ (98%, Chem Supply), $Cu(NO_3)_2.2½H_2O$ (98%, APS), KCl (99.5%, BDH Analar), HNO_3 (70%, Merck).

Materials used for the catalyst reactions and kinetic studies included allyl alcohol (99%, Riedel-de Haën), 2-methyl-2-propen-1-ol (98%, Fluka), *trans*-crotyl alcohol (96%, Sigma-Aldrich, 96% *trans* isomer), 3-methyl-2-buten-1-ol (99%, Sigma-Aldrich), geraniol (98%, Sigma-Aldrich), cinnamyl alcohol (98%, Alfa Aesar), *trans*-2-penten-1-ol (95%, Sigma-Aldrich), *cis*-2-penten-1-ol (97%, Alfa Aesar), *trans*-2-hexen-1-ol (97%, Alfa Aesar), *cis*-2-hexen-1-ol (94%, Alfa Aesar), allyl ethyl ether (95%, Sigma-Aldrich), 1,2-dichloethane (ACS reagent, ≥99%, Sigma-Aldrich), *t*-butylbenzene (99%, Sigma-Aldrich), H_2O_2 (~30% aqueous solution, Chem Supply), NaI (99.5%, Chem Supply), 2-propanol (99.7%, Chem Supply), glacial acetic acid (100%, BDH Analar), $Na_2S_2O_3.5H_2O$ (Merck, AR Grade, ≥99.0%) and Aliquat 336 (methyltrioctylammonium chloride, 96%, Sigma-Aldrich).

Solid state infrared spectra (IR) were obtained using a Perkin Elmer Spectrum BX instrument as KBr discs (resolution of $2\,cm^{-1}$). UV–visible-near infrared spectra were recorded on a Cary 6000i instrument from 1800 to 300 nm. Solution spectra were obtained using 1 cm quartz cells, while diffuse reflectance spectra were obtained with a Harrick praying mantis attachment. Thermogravimetric/differential thermal analyses (TG/DTA) were performed on a Perkin Elmer Diamond TG/DTA instrument. Sample masses of 10–20 mg were routinely used, with a heating rate of 10 °C/min and were performed in a flowing air atmosphere (20 mL/min).

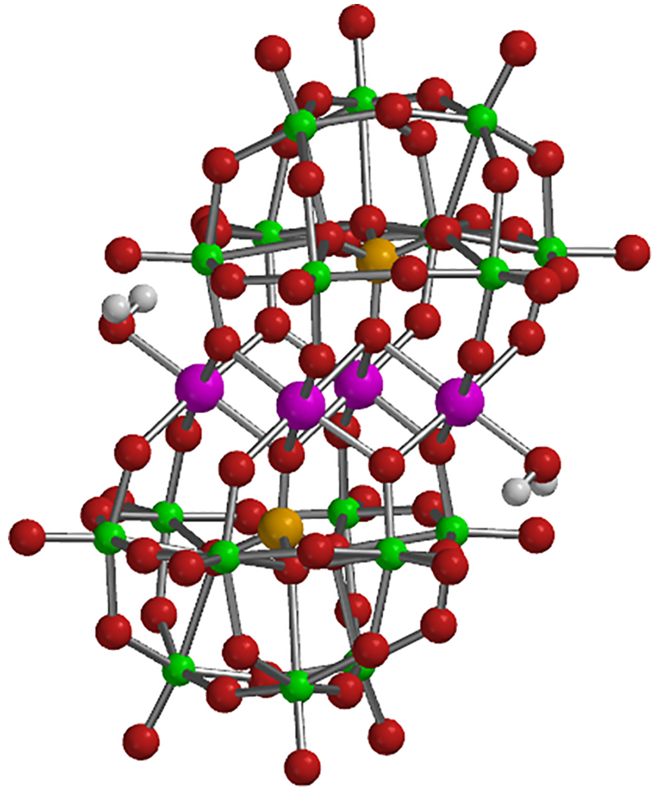

Fig. 3. A representation of an $[M_4(OH_2)_2(B\text{-}PW_9O_{34})_2]^{10-}$ anion. Colours: pink, M; green, W; orange, P; red, O; white, H. (For interpretation of the references to colour in this figure legend, the reader is referred to the web version of this article.)

2.1.2. Synthesis and characterization of the compounds $K_6Na[Ni_3(OH_2)_3(B\text{-}PW_9O_{34})\{WO_5(H_2O)\}].13H_2O$, $K_{12}[Co_3(OH_2)_6(A\text{-}PW_9O_{34})_2].18H_2O$ and $(cation)_{10}[M_4(OH_2)_2(B\text{-}PW_9O_{34})_2].(15\text{–}23)H_2O$, where M = Mn(II), Co(II), Ni(II), Cu(II) and Zn(II)

The trimetallic compounds $K_6Na[Ni_3(OH_2)_3(B\text{-}PW_9O_{34})\{WO_5(H_2O)\}].13H_2O$ and $K_{12}[Co_3(OH_2)_6(A\text{-}PW_9O_{34})_2].18H_2O$ were prepared according to the procedures described by Clemente-Juan et al. and Knoth et al., respectively [30,31]. Compounds of the type $(cation)_{10}[M_4(OH_2)_2(B\text{-}PW_9O_{34})_2].(15\text{–}23)H_2O$, where M = Mn(II), Co(II), Ni(II), Cu(II) and Zn(II) were prepared as described by Gomez-Garcia et al. (Mn compound), Finke et al. (Co, Cu and Zn compounds) and Clemente-Juan et al. (Ni compound) [30,34,36].

2.2. Catalysis reactions

2.2.1. Catalyst stock solution preparation

Bulk heteropolyoxotungstate catalyst solutions were prepared by dissolving 0.050 mmol of the Na^+/K^+ or K^+ salt in 10–20 mL of water. Slight heating (~30–40 °C) was required to achieve dissolution in some cases. On cooling, each solution was transferred to a 100 mL separatory funnel, along with 5 mL of water to ensure complete transfer of the catalyst solution. To this solution was added exactly 10.00 mL by pipette of a 1,2-dichloroethane solution that contained 1.0 mmol of Aliquat 336 (20 equivalents). The amount of added Aliquat 336 was always kept constant, as quaternary ammonium cations are known to extract H_2O_2 into 1,2-dichloroethane [22]. The resulting mixture was shaken for about 5 min which caused the coloured aqueous phase to decolourise, indicating that the catalyst had transferred to the 1,2-dichloroethane phase. The two phases were allowed to separate overnight. In the case of a colourless Zn(II)-containing compound, shaking was continued for 10 min to ensure complete transfer of the catalyst to the organic phase. After phase separation the 1,2-dichloroethane solution containing the catalyst was transferred to a dry volumetric flask.

2.2.2. *Catalysis reactions and analysis of the products of reaction*

All catalysis reactions were performed in a biphasic 1,2-dichloroethane/aqueous H_2O_2 mixture using a 10 mL glass vial that was fitted with a plastic screw top and teflon-coated magnetic stir bar, which was stirred using a Corning immersible stir pad (Model No. 440837). The screw top had a pinhole to vent any oxygen buildup from dismutation of H_2O_2. Typically, a sample of catalyst (1.0 mL, 5 μmol, 20 equivalents of Aliquat 336) was transferred to a 5 mL volumetric flask, followed by 5.0 mmol of organic substrate (0.35–1.15 mL) and 2.5 mmol (0.39 mL) of *t*-butylbenzene (as an internal GC standard) and the solution made up to 5.00 mL with 1,2-dichloroethane. This procedure gave a constant concentration of 1 mM of catalyst for each reaction, with a constant substrate concentration of 1.000 M. The resulting solution was then transferred to the glass vial, and a 2-fold excess of aqueous H_2O_2 (~30% v/v, ~10 mmol, 1 mL, pH ~3.2) over organic substrate was added. This always resulted in a biphasic mixture. The mixture was stirred vigorously at the designated temperature for 3 h, after which time the phases were allowed to separate by standing (5 min). The organic phase, both prior to the addition of the aqueous H_2O_2 and following reaction after standing, was analyzed by direct injection into a gas chromatograph. For the lower molecular weight allylic alcohols allyl alcohol, 2-methyl-2-propen-1-ol and *trans*-crotyl alcohol, but less so for 3-methyl-2-buten-1-ol, some transfer of the alcohol to the aqueous phase took place during the reaction, which resulted in greater apparent reactivity. This was significantly reduced by adding KCl (0.30 g) and stirring for 1–2 min, before the phase separation stage and subsequent GC analysis. Gas-phase chromatographic analyses were performed on a Shimadzu 17A gas chromatograph with a 15 m AT-Aquawax capillary column, coupled to a Shimadzu C-R8A Chromatopac integrator as described previously [14].

On completion of a reaction the H_2O_2 consumption was analyzed according to the following procedure. A 0.10 mL sample of the aqueous phase was removed using a 0.10 mL gas-tight precision glass syringe (SGE, 100F-GT) and analyzed by iodometric titration in acidic 2-propanol with standard 0.100 M $Na_2S_2O_3$ according to the procedure of Mair and Hall [37].

2.3. *Kinetic studies*

Kinetic studies of the epoxidation of 3-methyl-2-buten-1-ol by H_2O_2 under biphasic conditions were performed using $[Ni_3(OH_2)_3(B\text{-}PW_9O_{34})\{WO_5(H_2O)\}]^{7-}$ and $[Co_3(OH_2)_6(A\text{-}PW_9O_{34})_2]^{12-}$ as the catalyst anions, allowing comparison with our previous studies on $[WZn\{Mn(OH_2)\}_2(B\text{-}ZnW_9O_{34})_2]^{12-}$ as the catalyst [14].

A typical organic solution makeup consisted of 5 μmol of catalyst, 20 μmol of Aliquat 336, 5 mmol of 3-methyl-2-buten-1-ol (0.51 mL) and 2.5 mmol of *t*-butylbenzene (0.39 mL), all made up to 5.00 mL in 1,2-dichloroethane, and which was subsequently homogenized by shaking. Reaction was initiated by addition of a mixture of 20 mmol (2.00 mL) of 30% aqueous H_2O_2 and 2.00 mL of H_2O (pH 7). A biphasic mixture always resulted. For the catalyst and H_2O_2 concentration dependence studies the amounts of catalyst and H_2O_2/H_2O were varied accordingly. The reaction was studied by GC, as described above. Sampling occurred every 15 min, and the experimental conditions were adjusted to give sufficient data points for subsequent analysis. Temperature studies were performed from 15.0 to 35.0 °C for $[Ni_3(OH_2)_3(B\text{-}PW_9O_{34})\{WO_5(H_2O)\}]^{7-}$ and 1.0 to 15.0 °C for $[Co_3(OH_2)_6(A\text{-}PW_9O_{34})_2]^{12-}$. The catalyst concentrations were varied from 0.25 to 2.00 mM, while the aqueous H_2O_2 concentration was varied from ~ 2.13 to ~ 8.60 M. The kinetic data were analysed using an in-house extended version of ReactLab Kinetics [38].

3. Results and discussion

3.1. *Synthesis and characterization of $K_6Na[Ni_3(OH_2)_3(B\text{-}PW_9O_{34})\{WO_5(H_2O)\}].13H_2O$, $K_{12}[Co_3(OH_2)_6(A\text{-}PW_9O_{34})_2].18H_2O$ and $(cation)_{10}[M_4(OH_2)_2(B\text{-}PW_9O_{34})_2].(15\text{–}23)H_2O$, where M = Mn(II), Co(II), Ni(II), Cu(II) and Zn(II)*

All heteropolyoxotungstate compounds were prepared according to literature procedures, including the precursor compounds $A\text{-}Na_8H(PW_9O_{34}).24H_2O$ and $B\text{-}Na_8H(PW_9O_{34}).8H_2O$ (water content determined by TG/DTA) [39,40]. The resulting compounds were characterized by TG/DTA, and both IR and UV–visible spectroscopy. The TG/DTA and spectroscopic data are given in the Supplementary Material, Tables S1–S5 and Figs. S1–S3, and where available agree with the published data. In particular, the compound formulated by Knoth et al. as $K_{12}[Co_3(OH_2)_3(A\text{-}PW_9O_{34})_2].10H_2O$ [31], was found in our case to have twenty-four thermally-removable water molecules (up to 240 °C, Supplementary Material, Tables s4), and is better formulated as $K_{12}[Co_3(OH_2)_6(A\text{-}PW_9O_{34})_2].18H_2O$. Thus the anion is formally $[Co_3(OH_2)_6(A\text{-}PW_9O_{34})_2]^{12-}$, as shown in Fig. 2, containing three six-coordinate Co(II) with three externally coordinated water molecules, one to each of the three Co(II) in the waist of the anion, and three internally coordinated water molecules (as proposed by Knoth et al. [31]), again with one attached to each of the three Co(II). In Fig. 2 the anion structure has been based on that of the related $[Cu_3(NO_3)(A\text{-}PW_9O_{34})_2]^{13-}$ ion [41], but with Co···Co distances set at 5.356 Å, which is the same as the average Cu···Cu distance in the Cu_3-containing anion. In this last anion, there is an internally coordinated NO_3^- ion (rather than three water molecules), but no externally coordinated H_2O molecules (the three Cu(II) are each 5-coordinate), presumably because the externally directed 6th coordination site around each Cu(II) is vacant from weaker bonding as a result of the Jahn-Teller effect, with the two elongated *trans* bonds on each Cu(II) directed towards an oxygen atom of the internally coordinated NO_3^- group as well as (at least formally) radially outwards. In the $[Co_3(OH_2)_6(A\text{-}PW_9O_{34})_2]^{12-}$ ion, the three external Co(II) sites must be accessible by H_2O and allylic alcohol for the reaction mechanism to apply (see below), as the terminal W = O sites, which generate the $W(O_2)$ sites on reaction with H_2O_2, are located on the outside of the anion and are not available to the internally coordinated Co(II) sites. Also note that in Fig. 2 there are several long O···H bonds between the coordinated water molecules in the internal cavity (2.35–2.37 Å).

3.2. *The trimetallic $[Ni_3(OH_2)_3(B\text{-}PW_9O_{34})\{WO_5(H_2O)\}]^{7-}$ and $[Co_3(OH_2)_6(A\text{-}PW_9O_{34})_2]^{12-}$ ions*

3.2.1. *Comparative catalytic activity studies of the trimetallic $[Ni_3(OH_2)_3(B\text{-}PW_9O_{34})\{WO_5(H_2O)\}]^{7-}$ and $[Co_3(OH_2)_6(A\text{-}PW_9O_{34})_2]^{12-}$ ions*

A series of reactions using the $[Ni_3(OH_2)_3(B\text{-}PW_9O_{34})\{WO_5(H_2O)\}]^{7-}$ and $[Co_3(OH_2)_6(A\text{-}PW_9O_{34})_2]^{12-}$ ions, with a range of allylic alcohols and related compounds, which has been used previously for a comparison of the catalytic activities of the related $[WZn\{M(OH_2)\}_2(B\text{-}ZnW_9O_{34})_2]^{12-}$ ions, where M = Mn(II), Co(II), Ni(II), Cu(II) and Zn(II), was studied under identical conditions of concentration and temperature, etc., to that reported in the published study [14]. This allows a direct comparison with the earlier results. The catalytic activity results are shown in Table 1, along with the results for the $[WZn\{Mn(OH_2)\}_2(B\text{-}ZnW_9O_{34})_2]^{12-}$ ion (the reaction data for the analogous Co(II), Ni(II), Cu(II) and Zn(II) species can be found in [14]). Also included in Table 1 are the % H_2O_2 efficiency and the turnover frequency (TOF, h^{-1}), which is defined as the number of moles of product per mole of catalyst per hour. All reactions exhibited less than 100% efficiency in H_2O_2 consumption, as a result of the competitive dismutation of H_2O_2 (i.e. $2H_2O_2 \rightarrow 2H_2O + O_2$), arising from the heterotransition metal ions. The efficiency of H_2O_2 consumption varied widely, but there was no apparent relationship between the efficiency of H_2O_2 consumption with either the metal ion or the allylic alcohol.

Table 1
Oxidation of allylic alcohols by 30% aqueous H_2O_2 using the $[Ni_3(OH_2)_3(B\text{-}PW_9O_{34})\{WO_5(H_2O)\}]^{7-}$ and $[Co_3(OH_2)_6(A\text{-}PW_9O_{34})_2]^{12-}$ ions in biphasic 1,2-dichloroethane/H_2O at 15 °C. The corresponding data for the $[WZn\{Mn(OH_2)\}_2(B\text{-}ZnW_9O_{34})_2]^{12-}$ ion under the same conditions are included [14].

Substrate	Anion[a] % conversion, % H_2O_2 efficiency, TOF (h^{-1}), % aldehyde		
	$[Ni_3(OH_2)_3(B\text{-}PW_9O_{34})\{WO_5(H_2O)\}]^{7-}$	$[Co_3(OH_2)_6(A\text{-}PW_9O_{34})_2]^{12-}$	$[WZn\{Mn(OH_2)\}_2(B\text{-}ZnW_9O_{34})_2]^{12-}$
allyl alcohol	6, 22, 18, < 0.5	29, 43, 96, < 0.5	26, 68, 86, < 1
2-methyl-2-propen-1-ol	13, 43, 43, < 0.5	51, 44, 171, < 0.5	40, 72, 134, < 1
trans-crotyl alcohol	27, 36, 90, < 0.5	73, 56, 243, < 0.5	76, 82, 252, < 1
3-methyl-2-buten-1-ol	64, 94, 214, < 0.5	99, 73, 331, < 0.5	94, 74, 314, < 1
geraniol[b]	36, 98, 133, < 0.5	94, 64, 375, 1	77, 97, 306, 3
cinnamyl alcohol	23, 78, 77, < 0.5	48, 51, 159, 3	41, 68, 137, 4
trans-2-hexen-1-ol	28, 71, 93, 1[c]	33, 42, 108, 1	25, 48, 82, 2
cis-2-hexen-1-ol	17, 64, 56, 1[c]	38, 32, 126, 1	3, 30, 10, < 0.5
trans-2-penten-1-ol[d]	37, 78, 123, < 0.5[c]	46, 48, 153, 1	43, 46, 144, 2
cis-2-penten-1-ol[d]	45, 74, 150, < 0.5[c]	44, 38, 146, < 0.5	27, 29, 89, 1
allyl ethyl ether	NR[e]	NR	NR

[a] Reaction conditions: Reactions were carried out at 15 °C for 3 h using 5 mmol of allylic alcohol, 2.5 mmol of *t*-butylbenzene (internal standard for gas chromatography), 5 µmol of catalyst, 20 µmol of Aliquat 336 and 10 mmol of H_2O_2.

[b] Reaction conditions: as above, but reactions for 2.5 h.

[c] Reaction conditions: as above, but reaction at 25 °C.

[d] Data for $[WZn\{Mn(OH_2)\}_2(B\text{-}ZnW_9O_{34})_2]^{12-}$ from [42].

[e] NR = No reaction.

The relative reactivities of the allylic substrates have been comprehensively discussed previously [14,15]. Briefly, increasing substitution around the C═C by, for example, –CH_3 groups (reactions of allyl alcohol, 2-methyl-2-propen-1-ol, *trans*-crotyl alcohol and 3-methyl-2-buten-1-ol) demonstrated increases in catalytic activity, which can be correlated with the decreasing stability of the HOMO [14]. Geraniol (*trans*-3,7-dimethyl-2,6-octadien-1-ol) showed epoxidation only at the C═C site proximate to the –OH group, demonstrating high regioselectivity in these reactions. Cinnamyl alcohol (*trans*-3-phenyl-2-propen-1-ol) was less reactive than the structurally similar *trans*-crotyl alcohol, and always resulted in a small amount of cinnamaldehyde. A steric effect of the large phenyl group is likely to play a role in reactions of this substrate.

Of more interest are the reactions of the *trans*- and *cis*-pentenols and the *trans*- and *cis*-hexenols. In the absence of a catalyst, epoxidation usually occurs more readily for the *cis*-isomer, based on the energies of the HOMOs [14]. However, for $[WZn\{Mn(OH_2)\}_2(B\text{-}ZnW_9O_{34})_2]^{12-}$ it was observed previously that the *trans*-isomer was much more reactive than the *cis*-isomer for both the *trans*- and *cis*-pentenols and the *trans*- and *cis*-hexenols [14,42], which suggests a steric role for the catalyst at the Mn(II) site where the allylic alcohol coordinates. Notably, an identical order of activity was observed for the *trans*- and *cis*-hexenols with the other four $[WZn\{M(OH_2)\}_2(B\text{-}ZnW_9O_{34})_2]^{12-}$ ions, where M = Co(II), Ni(II), Cu(II) and Zn(II) [14]. However, for $[Ni_3(OH_2)_3(B\text{-}PW_9O_{34})\{WO_5(H_2O)\}]^{7-}$ and $[Co_3(OH_2)_6(A\text{-}PW_9O_{34})_2]^{12-}$ the patterns of *trans*:*cis* activity were observed to be somewhat different to those found for the five $[WZn\{M(OH_2)\}_2(B\text{-}ZnW_9O_{34})_2]^{12-}$ ions, as well as to each other (Table 1). This confirms that the environment around the M(II) site in these sandwich-type anions, where the allylic alcohol coordinates, imposes a steric effect on the epoxidation reaction, assuming the same reaction mechanism (see below). The $[Ni_3(OH_2)_3(B\text{-}PW_9O_{34})\{WO_5(H_2O)\}]^{7-}$ and $[Co_3(OH_2)_6(A\text{-}PW_9O_{34})_2]^{12-}$ ions are both much more open at their M(II) active sites than are the five $[WZn\{M(OH_2)\}_2(B\text{-}ZnW_9O_{34})_2]^{12-}$ ions (compare Figs. 1–3), such that the ratio of activity for the *cis* isomers relative to the *trans* isomers increases, and in some cases actually exceeds that of the *trans* isomers.

A substrate that has an oxygen atom in the same relative position to the C═C of the allylic alcohols but does not contain an –OH group is allyl ethyl ether. However, this did not show any reaction with H_2O_2 using either trimetallic catalyst, and demonstrates the importance of the –OH group to the reaction mechanism. Note that not one of the five $[WZn\{M(OH_2)\}_2(B\text{-}ZnW_9O_{34})_2]^{12-}$ ions acted as a catalyst for the reaction of allyl ethyl ether with H_2O_2 under the same conditions [14].

Of more importance for the present study, it is noted that for the three anions listed in Table 1, the order of catalytic activity is observed to be $[Co_3(OH_2)_6(A\text{-}PW_9O_{34})_2]^{12-}$ > $[WZn\{Mn(OH_2)\}_2(B\text{-}ZnW_9O_{34})_2]^{12-}$ > $[Ni_3(OH_2)_3(B\text{-}PW_9O_{34})\{WO_5(H_2O)\}]^{7-}$.

3.2.2. Kinetic studies of the trimetallic $[Ni_3(OH_2)_3(B\text{-}PW_9O_{34})\{WO_5(H_2O)\}]^{7-}$ and $[Co_3(OH_2)_6(A\text{-}PW_9O_{34})_2]^{12-}$ ions in the epoxidation of 3-methyl-2-buten-1-ol using aqueous H_2O_2

Kinetic studies of the epoxidation of 3-methyl-2-buten-1-ol by H_2O_2 under biphasic conditions (in 1,2-dichloroethane/H_2O) using the trimetallic $[Ni_3(OH_2)_3(B\text{-}PW_9O_{34})\{WO_5(H_2O)\}]^{7-}$ and $[Co_3(OH_2)_6(A\text{-}PW_9O_{34})_2]^{12-}$ ions as catalysts were undertaken, as these offer the possibility of a greater number of active sites compared to the previously examined $[WZn\{Mn(OH_2)\}_2(B\text{-}ZnW_9O_{34})_2]^{12-}$ ion [14]. As was found for this last species, all kinetic traces for the two trimetallic anions showed induction periods (see below), suggesting a similar reaction mechanism to that of the $[WZn\{Mn(OH_2)\}_2(B\text{-}ZnW_9O_{34})_2]^{12-}$ ion, albeit with three active metal sites rather than two. The reaction mechanism involves the exchange of the coordinated water on an M(II) by allylic alcohol (which coordinates through the –OH group), formation of a $W(O_2)$ group at an adjacent site by reaction of a W = O unit with H_2O_2, transfer of the peroxy oxygen to the coordinated allylic alcohol, followed by loss of the coordinated epoxide. Further discussion is given below. The Ni-OH_2 distances in the $[Ni_3(OH_2)_3(B\text{-}PW_9O_{34})\{WO_5(H_2O)\}]^{7-}$ catalyst range from 2.09(2) to 2.10(2) Å, which are slightly long for a Ni-OH_2 distance (typically 2.06 Å) so that the water will readily exchange with another ligand. The structure of the $[Co_3(OH_2)_6(A\text{-}PW_9O_{34})_2]^{12-}$ ion, while it has not been reported, has been discussed above and it is assumed that the externally-directed Co-OH_2 bonds will also exchange readily as Co(II) is a highly labile first row transition metal ion.

As an example of the formation of peroxy species as part of the reaction mechanism, the IR spectroscopic approach that was used previously for the detection of peroxo species of $[WZn\{Mn(OH_2)\}_2(B\text{-}ZnW_9O_{34})_2]^{12-}$ was employed to examine peroxo formation in $[Ni_3(OH_2)_3(B\text{-}PW_9O_{34})\{WO_5(H_2O)\}]^{7-}$ [14]. The results are shown in the Supplementary Material, Fig. S4. The figure shows the IR spectra from 1200 to 600 cm^{-1} of Aliquat 336, the parent $[Ni_3(OH_2)_3(B\text{-}PW_9O_{34})\{WO_5(H_2O)\}]^{7-}$ ion, and the latter following treatment with 15% H_2O_2 after 1 and 2 h. Note that the splitting of the υ(P—O) band observed for $[Ni_3(OH_2)_3(B\text{-}PW_9O_{34})\{WO_5(H_2O)\}]^{7-}$ in Fig. S1 cannot be observed in Fig. S4(b), 1042 cm^{-1}, which is likely the result of the type of sample preparation. All bands in the spectrum arise from the anion or Aliquat 336. Bands at 1059 (strong), 894 (medium) and 722 (strong) cm^{-1} may be observed for Aliquat 336 in Fig. S4(a). The peaks at 1059 and 722 cm^{-1} are observed also in the spectra of the anion treated with H_2O_2, Fig. S4(c) and (d), with the band at 722 cm^{-1} overlapping with the broad υ(W–O–W) band from the edge-shared WO_6 octahedra of the anion. On treatment with H_2O_2, formation of a peroxo band, υ(O—O), can be observed at 824 cm^{-1}, which grows with time. This is likely a W(η^2-O_2) site, based on the frequency [14]. There is also some shift in the positions of the υ(W═O) bands found at 954 and 937 cm^{-1} in the parent compound, to 962 and 947 cm^{-1}, with the higher frequency peak becoming more intense than the lower frequency peak. However, it cannot be determined as to where the peroxidation is occurring. This could occur at W═O sites of the $[B\text{-}PW_9O_{34}]^{9-}$ anion, or at the formal $[WO_5(H_2O)]^{4-}$ capping site, as the latter has two terminal W═O bonds.

The kinetic traces for the dependence of the reaction on the $[Ni_3(OH_2)_3(B\text{-}PW_9O_{34})\{WO_5(H_2O)\}]^{7-}$ and H_2O_2 concentrations (both at 25 °C), as well as the temperature dependence study (15–35 °C) are shown in Figs. 4–6, respectively. For $[Co_3(OH_2)_6(A\text{-}PW_9O_{34})_2]^{12-}$ the traces for catalyst concentration dependence (5 °C) and temperature dependence (1–15 °C) are shown in the Supplementary Material, Figs. S5 and S6. The figures show the dependence of the reactions as plots of the residual 3-methyl-2-buten-1-ol concentration vs time. In general, all reactions were followed until about 50–60% conversion of the 3-methyl-2-buten-1-ol. This was imposed on the study, as it has been shown that, in related systems, the build-up of product epoxide can lead to decomposition of the catalyst [43]. A similar restriction was likewise applied in the study of the $[WZn\{Mn(OH_2)\}_2(B\text{-}ZnW_9O_{34})_2]^{12-}$ ion as catalyst [14].

The induction period depended on the concentrations of the catalyst and H_2O_2 (the latter was only studied for the $[Ni_3(OH_2)_3(B\text{-}PW_9O_{34})\{WO_5(H_2O)\}]^{7-}$ ion), as well as the temperature. Similar findings were found for the analogous studies of the $[WZn\{Mn(OH_2)\}_2(B\text{-}ZnW_9O_{34})_2]^{12-}$ ion as catalyst [14]. The reactions involving this latter anion were interpreted in terms of an autocatalysis reaction, as this anion was known to be stable under the reaction conditions. In the present case a comprehensive set of reaction steps that account for such a mechanism is given below, equations (1) to (21), but unlike the two-site $[WZn\{Mn(OH_2)\}_2(B\text{-}ZnW_9O_{34})_2]^{12-}$ ion, three sites were used for the trimetallic $[Ni_3(OH_2)_3(B\text{-}PW_9O_{34})\{WO_5(H_2O)\}]^{7-}$ and $[Co_3(OH_2)_6(A\text{-}PW_9O_{34})_2]^{12-}$ ions, which extended the number of reaction steps from fourteen to twenty-one. The twenty-one steps in the mechanism can be classified according to the following scheme.

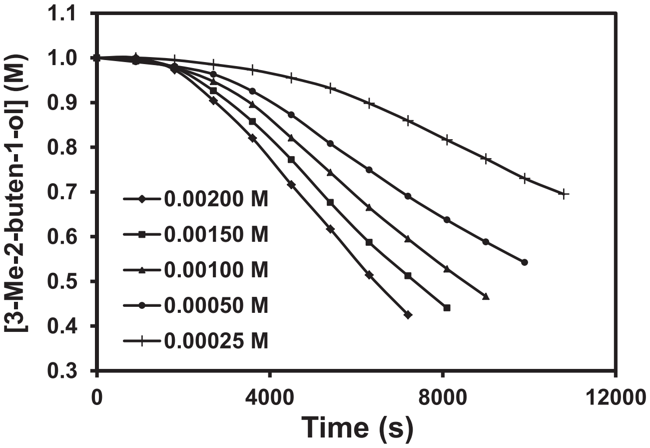

Fig. 4. Catalyst ($[Ni_3(OH_2)_3(B\text{-}PW_9O_{34})\{WO_5(H_2O)\}]^{7-}$) concentration dependence: plot of residual 3-methyl-2-buten-1-ol concentration versus time for the epoxidation of 3-methyl-2-buten-1-ol by H_2O_2 at 25 °C: [3-methyl-2-buten-1-ol] = 1.000 M, $[H_2O_2]$ = 4.50 M, [Aliquat 336] = 0.020 M.

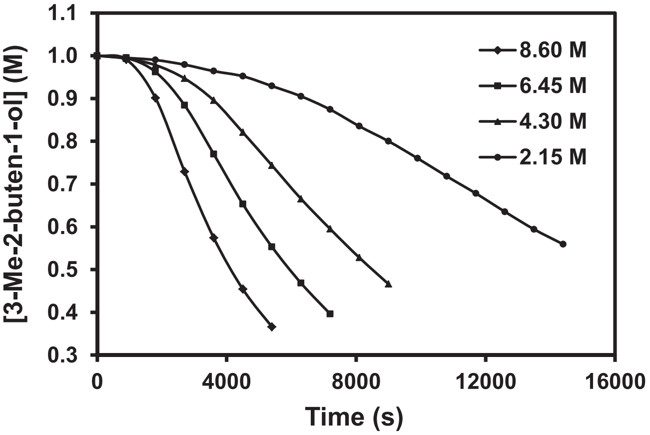

Fig. 5. H_2O_2 concentration dependence: plot of residual 3-methyl-2-buten-1-ol concentration versus time for the epoxidation of 3-methyl-2-buten-1-ol at 25 °C: [3-methyl-2-buten-1-ol] = 1.000 M, catalyst $[Ni_3(OH_2)_3(B\text{-}PW_9O_{34})\{WO_5(H_2O)\}^{7-}]$ = 1.00 mM, [Aliquat 336] = 0.020 M.

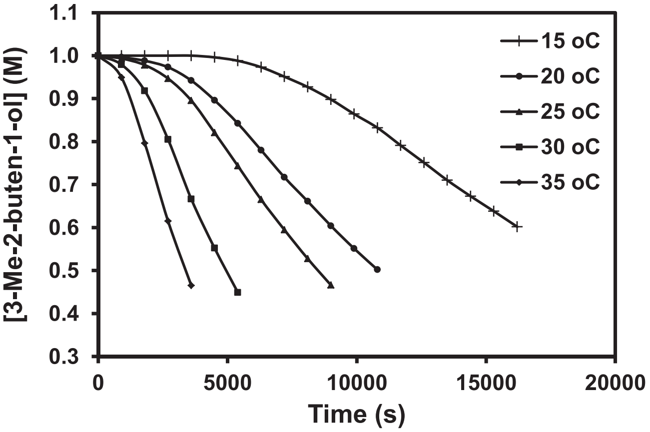

Fig. 6. Temperature dependence (15–35 °C): plot of residual 3-methyl-2-buten-1-ol concentration versus time for the epoxidation of 3-methyl-2-buten-1-ol: [3-methyl-2-buten-1-ol] = 1.000 M, catalyst $[Ni_3(OH_2)_3(B\text{-}PW_9O_{34})\{WO_5(H_2O)\}^{7-}]$ = 1.00 mM, [Aliquat 336] = 0.020 M.

(a) Preliminary equilibria (coordination of C_3 by A):

$$C_3 + A \leftrightharpoons C_3A \quad (K_1) \tag{1}$$

$$C_3A + A \leftrightharpoons C_3A_2 \quad (K_2) \tag{2}$$

$$C_3A_2 + A \leftrightharpoons C_3A_3 \quad (K_3) \tag{3}$$

(b) Peroxo formation; oxygen transfer and associated equilibria:

$$C_3A_3 + O \rightarrow C_3A_3O \quad (k_4) \tag{4}$$

$$C_3A_3O \rightarrow C_3A_2E \quad (k_5) \tag{5}$$

$$C_3A_2 + E \leftrightharpoons C_3A_2E \quad (K_6) \tag{6}$$

$$C_3A_2 + O \rightarrow C_3A_2O \quad (k_7) \tag{7}$$

$$C_3A_2O \rightarrow C_3AE \quad (k_8) \tag{8}$$

$$C_3A + E \leftrightharpoons C_3AE \quad (K_9) \tag{9}$$

(c) Autocatalysis and sundry reactions:

$$C_3A_2E + O \rightarrow C_3A_2ES \quad (k_{10}) \tag{10}$$

$$C_3A_2S + E \leftrightharpoons C_3A_2ES \quad (K_{11}) \tag{11}$$

$$C_3A_2S + A \leftrightharpoons C_3A_3O \quad (K_{12}) \tag{12}$$

(Note, C_3A_3O formation in equation (12) is followed by equation (5) above, while an S oxygen becomes an O oxygen when the coordinated E is lost and replaced with an A);

$$C_3AE + O \rightarrow C_3AES \quad (k_{13}) \tag{13}$$

$$C_3AS + E \leftrightharpoons C_3AES \quad (K_{14}) \tag{14}$$

$$C_3AS + A \leftrightharpoons C_3A_2O \quad (K_{15}) \tag{15}$$

(Note, C_3A_2O formation in equation (15) is followed by equation (8) above, while an S oxygen becomes an O oxygen when the coordinated E is lost and replaced with an A);

$$C_3A_2E + O \rightarrow C_3A_2EO \quad (k_{16}) \tag{16}$$

$$C_3A_2EO \rightarrow C_3AE_2 \quad (k_{17}) \tag{17}$$

$$C_3AE + E \leftrightharpoons C_3AE_2 \quad (K_{18}) \tag{18}$$

$$C_3AE + O \rightarrow C_3AEO \quad (k_{19}) \tag{19}$$

$$C_3AEO \rightarrow C_3E_2 \quad (k_{20}) \tag{20}$$

$$C_3E + E \leftrightharpoons C_3E_2 \quad (K_{21}) \tag{21}$$

The equilibrium and rate constants are numbered successively from 1 to 21, with the equilibrium constants designated by K and the rate constants by k. These are shown in parentheses to the right of the reaction in each step of the mechanism in equations (1) to (21). A double arrow ($\leftrightharpoons$) represents an equilibrium that is regarded as kinetically very fast on the scale of the overall epoxidation reaction, while a single arrow ($\rightarrow$) is a kinetically observable reaction.

In the above equations C_3 represents the three metal sites of the anion (with C representing a single metal site) and A is the allylic alcohol. Thus C_3A represents coordination of an allylic alcohol to a single metal site (so that C_3A_2 and C_3A_3 represent coordination of 2 and 3 metal sites, respectively). O is the "peroxo" atom of an H_2O_2 molecule, and addition of O indicates formation of a $W(O_2)$ peroxo site in the anion that is adjacent to a coordinated allylic alcohol, which is then capable of transferring an O atom to the C=C bond of the coordinated allylic alcohol in a separate step (note that the H_2O_2 reduction product H_2O is not represented in these equations). The product hydroxy epoxide E is also able to coordinate to a metal center C through its –OH group, as does the allylic alcohol. Note that E is different from AO, as AO represents separated A and O entities that have yet to combine to give the product hydroxy epoxide E. S represents formation of a $W(O_2)$ peroxo site that is adjacent to a coordinated hydroxy epoxide, and so cannot react until the hydroxy epoxide has been replaced by an allylic alcohol. The formation of C_3A_3, C_3A_2 and C_3A are required as at the concentrations used, the three M(II) sites (i.e. C_3) are almost fully coordinated by A at the beginning of the reaction (~99.8%, with a $[C_3A_3]$:$[C_3A_2]$:$[C_3A]$ ratio of 39.6:8.9:1 for the trimetallic Ni(II) system, and 19.8:6.3:1 for the trimetallic Co(II) system, using the chosen values of K_1, K_2 and K_3 for each of the trimetallic systems; see below). At the end of the reaction, equations for the formation of C_3E_3, C_3E_2 and C_3E would also be required, but as all catalysis reactions were followed only to 50–60% conversion the formation of C_3E_3 was neglected (also see the discussion below). The steps in the mechanism consist only of equilibria based on coordination of allylic alcohol and hydroxy epoxide to Ni(II) or Co(II), formation of tungsten(VI)-peroxo sites, and transfer of oxygen from a peroxo site to the C=C bond of the coordinated allylic alcohol.

The twenty-one steps listed above comprise only a subset of all possible reactions that can be written in a three-site system. However, many of the full set of equations are either unnecessary or are not required to successfully describe the observed kinetics. This was also found for the kinetic study of the epoxidation of 3-methyl-2-buten-1-ol by H_2O_2 under biphasic conditions (1,2-dichloroethane/H_2O) using the two-site $[WZn\{Mn(OH_2)\}_2(B\text{-}ZnW_9O_{34})_2]^{12-}$ ion as the catalyst [14]. Thus, in the present case, the four species C_3A, C_3A_2, C_3AE and C_3A_2E comprise a 4-species cyclic system, whereby C_3A can react either with A first and then E, or with E first and then A, with both pathways resulting in C_3A_2E formation. ReactLab Kinetics only requires three sets of equilibrium equations (equations (2), (6) and (9)), along with their equilibrium constants, to be defined for a 4-species cyclic system. The program automatically generates the fourth equilibrium, in this case the reaction between C_3AE and A to generate C_3A_2E. The equilibrium constant for this reaction is calculated by microscopic reversibility/detailed balancing from the three defined equilibrium constants [14,44]. Also, using the chosen equilibrium constants (see below), any reaction of C_3 with O to give C_3O can be neglected. The concentrations of C_3 in both the $[Ni_3(OH_2)_3(B\text{-}PW_9O_{34})\{WO_5(H_2O)\}]^{7-}$ system and the $[Co_3(OH_2)_6(A\text{-}PW_9O_{34})_2]^{12-}$ system are 1.1×10^{-3} and 2.9×10^{-3} mM, respectively (both for an initial $[C_3] = 1.00$ mM and $[A] = 1.000$ M), which are much lower than fully or partially complexed C_3. In addition, as the equilibria can be regarded as "instantaneous" compared to the kinetically observable rate constants, the reaction of C_3 with O to give C_3O prior to complexation with A or E may be neglected. Another reaction that was neglected was the reaction of C_3A with O, as the concentration of C_3A is much less than C_3A_2 and C_3A_3 (the concentrations of C_3A are only 2.0×10^{-2} mM and 3.7×10^{-2} mM in the Ni- and Co-trimetallic systems, respectively), so that the major reaction pathways proceed through C_3A_3 and C_3A_2. The reactions of C_3E_3, C_3AE_2 and C_3E_2 with O to give C_3E_3S, C_3AE_2S and C_3E_2S (recall that S is an O that generates a peroxo group adjacent to E) have also been neglected. Reaction can only occur if there is loss of E and addition of A. Because the catalysis reactions were only followed until a maximum of 50–60% conversion, the concentrations of C_3E_2 and C_3AE_2 only reach a maximum of ~0.14 and ~0.09 mM, respectively, with that of C_3E_3 much lower still, in the two trimetallic systems. Thus these reactions were not included in the reaction scheme above. Note, however, that if the catalysis studies were to be followed to much higher % conversions, then these reactions, along with their reactions for loss of E and addition of A, together with subsequent reactions (transfer of O to A and product formation) would have to be taken into account. The same approach was also applied successfully in our previous study using the two-site $[WZn\{Mn(OH_2)\}_2(B\text{-}ZnW_9O_{34})_2]^{12-}$ ion as catalyst [14]. Note also that C_3E, C_3AE, C_3E_2 and C_3AE_2 will form a 4-species cyclic system and due account of only three of the four possible reactions would need to be considered.

Because of the symmetrical nature of the trimetallic $[Ni_3(OH_2)_3(B\text{-}PW_9O_{34})\{WO_5(H_2O)\}]^{7-}$ and $[Co_3(OH_2)_6(A\text{-}PW_9O_{34})_2]^{12-}$ ions [29,30,41], several formation and rate constants can be regarded as being effectively related or even equivalent, as was also invoked in the analogous study of the $[WZn\{Mn(OH_2)\}_2(B\text{-}ZnW_9O_{34})_2]^{12-}$ ion as catalyst [14]. In the case of the rate constants for peroxo formation, k_4, k_7, k_{16} and k_{19} were assumed to be equal, as were k_{10} and k_{13}. For peroxo O transfer to an adjacent coordinated allylic alcohol, k_5, k_8, k_{17} and k_{20} were assumed to be equal.

No experimental values for the stepwise coordination of 3-methyl-2-buten-1-ol to $[Ni_3(OH_2)_3(B\text{-}PW_9O_{34})\{WO_5(H_2O)\}]^{7-}$ could be obtained. The molar absorptivities of the three observable Ni(II) d-d transitions were very low (see the Supplementary Material, Table S3) and the magnitudes of the stability constants were also expected to be low as well, based on our previous studies [14,15]. This makes their spectrophotometric determination effectively impossible. However, previously obtained experimental data is available that allows us to estimate a likely value. In this we follow a similar procedure to that used for the evaluation of the stability constant for the addition of 3-methyl-2-buten-1-ol to $[WZn\{Mn(OH_2)\}_2(B\text{-}ZnW_9O_{34})_2]^{12-}$ as used in our previous study [14]. Stability constants for allylic alcohols bound to the substituted Co(II) in the related Dawson anion $[P_2W_{17}O_{61}Co(Cl)]^{9-}$ in 1,2-dichloroethane at 25 °C vary from $19.0\ M^{-1}$ for allyl alcohol, $13.9\ M^{-1}$ for 2-methyl-2-propen-1-ol, $12.2\ M^{-1}$ for *trans*-crotyl alcohol, to 12.7 M^{-1} in 3-methyl-2-buten-1-ol. For the same four allylic alcohols the K_1 values for the analogous Mn(III)-substituted Dawson anion range from 14.2 to 10.4 M^{-1} [15]. These values do not involve deprotonation of the –OH group, and hence any formation of an M(n+)-alcoholate type species.

For the $[Ni_3(OH_2)_3(B\text{-}PW_9O_{34})\{WO_5(H_2O)\}]^{7-}$ ion, we have chosen to use a value of $K_1 = 17.7\ M^{-1}$ (i.e. log $K_1 = 1.25$) for a Ni(II) site coordinating a 3-methyl-2-buten-1-ol molecule at 25 °C in 1,2-dichloroethane for the present study, which was evaluated by taking the stability constant value for complexation of 3-methyl-2-buten-1-ol to Co(II) in the (structurally similar) Co(II)-substituted Dawson anion and scaling it upwards by 40%, so as to account for the natural order of stability constants (the Irving-Williams series). The scaling was based on relative stability constants for coordination of a neutral O donor (in this case H_2O) to Ni(II) relative to Co(II), made with the same experimental techniques and under the same experimental conditions [45,46]. This generates the value for K_1. However, it is unlikely that K_1, K_2 and K_3 are equal for all three Ni(II) sites, given that the Ni⋯Ni distances average only 3.176 Å in the $[Ni_3(OH_2)_3(B\text{-}PW_9O_{34})\{WO_5(H_2O)\}]^{7-}$ ion [29,30]. Some reduction in K_n values for successive complexation would likely arise from steric effects between the coordinating allylic alcohol molecules. Moreover, in the case of the two-site species $[Co_4(OH_2)_2(B\text{-}PW_9O_{34})_2]^{10-}$, for the N-donor *N*-methylimidazole, which has much greater stability constant values than the O-donor 3-methyl-2-buten-1-ol used in the present study, two ligand complexation steps have been observed with $K_2 < K_1$ [47]. We have thus chosen to successively decrease a K_{n+1} value relative to K_n by the factor 0.5, giving values of $K_2 = 8.9\ M^{-1}$ and $K_3 = 4.4\ M^{-1}$ for complexation of the three 3-methyl-2-buten-1-ol molecules to Ni(II). Using the same approach for $[Co_3(OH_2)_6(A\text{-}PW_9O_{34})_2]^{12-}$ (despite the fact that the Co⋯Co distance is certain to be larger, see above) the initial K_1 value was assumed to be the same as that for complexation of 3-methyl-2-buten-1-ol to Co(II) in the Co(II)-substituted Dawson anion, i.e. $K_1 = 12.7\ M^{-1}$, with $K_2 = 6.4\ M^{-1}$ and $K_3 = 3.2\ M^{-1}$. In the case of the Co(II) trimetallic system, no attempt was made to account for the difference in temperature at which the kinetic dependence on the catalyst concentration was determined and the stability constant data. However, this temperature difference should only lead to a small effect on the value of the stability constants [48]. While the final values of K_1, K_2 and K_3 in both trimetallic systems may be approximate in each case, some variation in their magnitudes will be discussed below. No analogous stability constants for complexation of the product hydroxy epoxide to Ni(II) or Co(II) are known (i.e. K_6, K_9, K_{11}, K_{14}, K_{18} and K_{21}), but these are likely to be similar to the analogous values for 3-methyl-2-buten-1-ol, so that the stability constants for 3-methyl-2-buten-1-ol and its epoxide were assumed equivalent for the respective values of K_1, K_2 and K_3 for both trimetallic systems. This is the same procedure that was used in the case of our previous study of the kinetics of the epoxidation of 3-methyl-2-buten-1-ol by H_2O_2 under biphasic conditions with $[WZn\{Mn(OH_2)\}_2(B\text{-}ZnW_9O_{34})_2]^{12-}$ as the catalyst [14].

With these simplifications in place, this leaves just k_4, k_5 and k_{10} to be determined for each trimetallic system. The results of the fitting of the GC data for both the catalyst and H_2O_2 concentration dependence studies are given in Tables 2 and 3 for the $[Ni_3(OH_2)_3(B\text{-}PW_9O_{34})\{WO_5(H_2O)\}]^{7-}$ ion and for the concentration dependence study for $[Co_3(OH_2)_6(A\text{-}PW_9O_{34})_2]^{12-}$, respectively. Also included in Tables 2 and 3 are the temperature dependence data for each trimetallic anion. For $[Ni_3(OH_2)_3(B\text{-}PW_9O_{34})\{WO_5(H_2O)\}]^{7-}$ a typical fitting of the calculated and experimental data for [catalyst] = 1.50 mM, $[H_2O_2]$ = 4.50 M and [3-methyl-2-buten-1-ol] = 1.000 M at 25.0 °C is shown in Fig. 7. The sum of the differences squared between the experimental and fitted data points (ssq) is 0.0008. The ssq values for the reactions in Table 2 varied from 0.0001 to 0.0010, and for the reactions in Table 3 from 0.0001 to 0.0004.

The three unique rate constants k_4, k_5 and k_{10} reported in Tables 2 and 3 for the eight [catalyst] and $[H_2O_2]$ dependence studies in Table 2 and the three [catalyst] studies in Table 3 should be individually constant, with differences evident between the Ni and Co trimetallic systems. The average values are given in both tables. In general, the rate constants for the concentration dependence studies are fairly constant for both the Ni and Co trimetallic systems. Thus k_4 is relatively constant, while some slight variations are observed for k_5 and k_{10} for the [catalyst] and $[H_2O_2]$ (Ni_3 system) and [catalyst] (Co_3 system) dependence studies. The variations may have several possible causes. Note that the studies were carried out in 1,2-dichloroethane solvent, and involved significant concentrations of ionic species (both catalyst and Aliquat 336, although the latter is actually constant throughout all studies), and high concentrations of neutral species (3-methyl-2-buten-1-ol, H_2O_2 and product hydroxy epoxide) in 1,2-dichloroethane. No activity coefficients could be applied during the numerical fitting process so that no account could be made for ionic strength which will vary in the [catalyst] studies or for the actual activities of the neutral solvent in all studies. This will likely have some effect on the fitted values of the rate constants and are likely the cause of the observed variations. Similar variations were observed previously for the related $[WZn\{Mn(OH_2)\}_2(B\text{-}ZnW_9O_{34})_2]^{12-}$ catalyst system. While k_4 and k_5 are fairly similar for both the Ni_3 and Co_3 catalyst systems, even allowing for the temperature difference, k_{10} is much faster in the Co_3 system. This likely arises from the ease of formation of the transition state in the autocatalytic pathway. Further comparisons are evident from the enthalpies of activation ($\Delta H^{\neq}$), entropies of activation ($\Delta S^{\neq}$) and free energies of activation at 25 °C ($\Delta G^{\neq}$), see below.

As discussed previously [14], the autocatalysis is caused by an increase in the rate of formation of a peroxo site that is adjacent to a coordinated hydroxy epoxide (k_{10} and k_{13}) relative to one adjacent to a coordinated allylic alcohol (k_4 and k_7). The steps that are involved in the autocatalysis (k_5, k_{10}, K_{11}, K_{12}, k_8, k_{13}, K_{14} and K_{15}) result in the acceleration of the overall rate with time following the induction period, as shown in Figs. 4–6, S5 and S6 and the increase in k_{10} (and k_{13}) relative to k_4 (and k_7), respectively, may again be attributed to an electronic (possibly inductive) effect from the coordinated hydroxy epoxide. Alternatively, the increase may be steric in nature, with the coordinated hydroxy epoxide actually directing formation of the adjacent peroxo group. The latter might be expected to depend on the environment surrounding the site where the allylic alcohol coordinates to the M(II), but no firm conclusions can be made considering the significantly different environments of the $[Co_3(OH_2)_6(A\text{-}PW_9O_{34})_2]^{12-}$, $[Ni_3(OH_2)_3(B\text{-}PW_9O_{34})\{WO_5(H_2O)\}]^{7-}$ and $[WZn\{Mn(OH_2)\}_2(B\text{-}ZnW_9O_{34})_2]^{12-}$ ions.

Variation of the K_1 value (and thus K_2, K_3, K_6, K_9, K_{11}, K_{12}, K_{14}, K_{15}, K_{18} and K_{21}) for the eleven equilibria by increasing its value (×2) or decreasing its value (×0.5) produced only relatively small changes in the values of k_4, k_5 and k_{10}. For example, for the trimetallic Ni(II) system with [catalyst] = 1.00 mM, [3-methyl-2-buten-1-ol] = 1.000 M, $[H_2O_2]$ = 4.50 M and T = 25 °C, increasing and decreasing K_1 (and K_2 and K_3) by the above factors gave variations for k_4 of −6 and +19%, respectively, k_5 of +9 and −15%, respectively, and k_{10} of +1 and −12%, respectively. Likewise, for the trimetallic Co(II) system with [catalyst] = 1.00 mM, [3-methyl-2-buten-1-ol] = 1.000 M, $[H_2O_2]$ = 2.125 M and T = 5 °C, the variations were for k_4 of −2 and −3%, respectively, k_5 of +6 and −23%, respectively, and k_{10} of +15 and −6%, respectively. In each case the choice made for K_1 does not have a strong bearing on the fitted rate constants.

Setting the three values of K_1, K_2 and K_3 equal within each of the trimetallic systems, with values for all log K_n = 1.25 for the Ni(II) system and all log K_n = 1.10 for the Co(II) system resulted in variations for k_4 of −9%, k_5 of +14% and k_{10} of +6%, for the former, and k_4 of −5% k_5 of +11% and k_{10} of +16% for the latter. Again the variations are not large, indicating that the choice of K_1 does not have a strong influence on the fitted rate constants. Attempts to fit the values of K_1, K_2 and K_3 along with the rate constants were unsuccessful, giving inconsistent results. It is assumed that the data are not sensitive (or extensive) enough to be able to refine both the equilibrium and rate constants.

For the temperature dependence data for both trimetallic systems (Tables 2 and 3) no variations in the values of K_1 (and K_2 and K_3) were made in either case, as the temperature dependence data of K_1 for

Table 2

Rate constants for the epoxidation of 3-methyl-2-buten-1-ol by H_2O_2 using the $[Ni_3(OH_2)_3(B\text{-}PW_9O_{34})\{WO_5(H_2O)\}]^{7-}$ ion as the catalyst under biphasic conditions (Aliquot 336/1,2-dichloroethane/H_2O).[a]

[catalyst] (M)	$[H_2O_2]$ (M)	Temperature (°C)	Rate Constants (standard deviations in the last figure in parentheses)		
			k_4 $(=k_7 = k_{16} = k_{19})(M^{-1}\,s^{-1})$	k_5 $(=k_8 = k_{17} = k_{20})(s^{-1})$	k_{10} $(=k_{13})$ $(M^{-1}\,s^{-1})$
A. [catalyst] and $[H_2O_2]$ dependence: [3-methyl-2-buten-1-ol] = 1.000 M					
0.00200	4.30	25	2.8 (2) × 10^{-4}	0.15 (1)	0.21 (1)
0.00150	4.30	25	2.8 (1) × 10^{-4}	0.17 (1)	0.26 (1)
0.00100	4.30	25	2.9 (1) × 10^{-4}	0.21 (1)	0.57 (1)
0.00050	4.30	25	2.8 (1) × 10^{-4}	0.25 (1)	0.92 (2)
0.00025	4.30	25	2.9 (2) × 10^{-4}	0.34 (1)	1.23 (1)
0.00100	2.15	25	3.1 (1) × 10^{-4}	0.09 (1)	0.47 (1)
0.00100	6.45	25	2.8 (1) × 10^{-4}	0.28 (1)	0.37 (1)
0.00100	8.60	25	2.7 (2) × 10^{-4}	0.39 (1)	0.42 (1)
Average:			**2.9 (1) × 10^{-4}**	**0.23 (9)**	**0.6 (3)**
B. Temperature dependence: [3-methyl-2-buten-1-ol] = 1.000 M					
0.00100	4.30	15	2.6 (1) × 10^{-4}	0.13 (1)	0.12 (1)
0.00100	4.30	20	2.8 (1) × 10^{-4}	0.16 (1)	0.31 (1)
0.00100	4.30	30	3.1 (5) × 10^{-4}	0.29 (1)	0.86 (1)
0.00100	4.30	35	3.2 (4) × 10^{-4}	0.38 (1)	1.60 (1)

[a] Equilibrium constants: $\log K_1 = 1.25$, $\log K_2 = \log K_9 = \log K_{14} = \log K_{15} = \log K_{21} = 0.95$, $\log K_3 = \log K_6 = \log K_{11} = \log K_{12} = \log K_{18} = 0.65$.

coordination of both 3-methyl-2-buten-1-ol and the hydroxy epoxide are unknown in each system. However, as the values of K_1 are small, the variations of this value for each system will only vary slightly [48] and, as shown above, the variations in the values of K_1, K_2 and K_3 have only a small effect on the fitted rate constants.

The resulting Eyring plots (ln k/T vs $1/T$) for k_4, k_5 and k_{10} for the trimetallic Ni(II) and Co(II) systems are given in the Supplementary Material, Figs. S7 to S9 and S10 to S12, respectively (with all $R^2 > 0.96$). The resulting thermodynamic data are summarised in Table 4, along with the analogous data for $[WZn\{Mn(OH_2)\}_2(B\text{-}ZnW_9O_{34})_2]^{12-}$ as catalyst, which were obtained under identical conditions to those used in the current study.

The large negative values of $\Delta S^{\neq}$ for k_4 and k_5 (k_3 and k_4 for the $[WZn\{Mn(OH_2)\}_2(B\text{-}ZnW_9O_{34})_2]^{12-}$ ion) likely indicate significant changes in solvation during these steps. The values of $\Delta G^{\neq}$ at 25 °C for all three anions show the reduction in k_{10} (k_9 for the two-site system), the autocatalytic pathway, relative to k_4 (k_3 for the two-site system), the non-autocatalytic pathway. The thermodynamic data are very similar for all three anions, which is not surprising as the reaction mechanism is the same in each case, albeit with a variation in the number of active sites. However, the $\Delta S^{\neq}$ value of k_{10} for $[Co_3(OH_2)_6(A\text{-}PW_9O_{34})_2]^{12-}$ is negative rather than positive, which may indicate significant differences in solvent redistribution during this step. This results in a smaller $\Delta G^{\neq}$ value at 25 °C for this anion, making it the most active catalyst of the three heteropolyoxotungstate anions that have been studied.

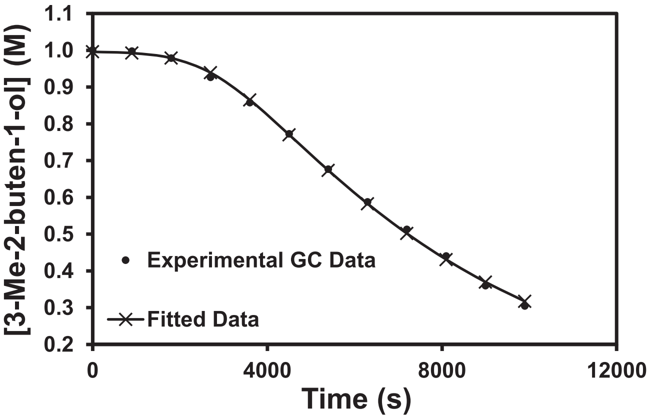

Fig. 7. Calculated (×) and experimental (•) GC results for the epoxidation of 3-methyl-2-buten-1-ol at 25 °C: [3-methyl-2-buten-1-ol] = 1.000 M, catalyst $[Ni_3(OH_2)_3(B\text{-}PW_9O_{34})\{WO_5(H_2O)\}^{7-}]$ = 1.50 mM, $[H_2O_2]$ = 4.50 M, [Aliquat 336] = 0.020 M. The ssq = 0.0008.

3.3. Comparative catalytic activity studies of the $[M_4(OH_2)_2(B\text{-}PW_9O_{34})_2]^{10-}$ ions, where M = Mn(II), Co(II), Ni(II), Cu(II) and Zn(II)

The series of sandwich-type heteropolyoxotungstate anions of composition $[M_4(OH_2)_2(B\text{-}PW_9O_{34})_2]^{10-}$ is directly related to the

Table 3

Rate constants for the epoxidation of 3-methyl-2-buten-1-ol by H_2O_2 using the $[Co_3(OH_2)_6(A\text{-}PW_9O_{34})_2]^{12-}$ ion as the catalyst under biphasic conditions (Aliquot 336/1,2-dichloroethane/H_2O).[a]

[catalyst] (M)	$[H_2O_2]$ (M)	Temperature (°C)	Rate Constants (standard deviations in the last figure in parentheses)		
			k_4 $(=k_7 = k_{16} = k_{19})$ $(M^{-1}\,s^{-1})$	k_5 $(=k_8 = k_{17} = k_{20})$ (s^{-1})	k_{10} $(=k_{13})$ $(M^{-1}\,s^{-1})$
A. [catalyst] dependence: [3-methyl-2-buten-1-ol] = 1.000 M					
0.00100	2.125	5	3.0 (1) × 10^{-4}	0.140 (1)	3.43 (9)
0.00050	2.125	5	2.9 (1) × 10^{-4}	0.161 (1)	4.14 (2)
0.00025	2.125	5	2.9 (1) × 10^{-4}	0.192 (1)	5.46 (5)
Average:			**2.9 (1) × 10^{-4}**	**0.16 (2)**	**4.3 (8)**
B. Temperature dependence: [3-methyl-2-buten-1-ol] = 1.000 M					
0.00100	2.125	1	2.9 (1) × 10^{-4}	0.098 (1)	2.29 (5)
0.00100	2.125	5	3.0 (1) × 10^{-4}	0.140 (1)	3.43 (9)
0.00100	2.125	10	3.1 (4) × 10^{-4}	0.206 (2)	5.4 (2)
0.00100	2.125	15	3.2 (9) × 10^{-4}	0.248 (1)	6.4 (5)

[a] Equilibrium constants: $\log K_1 = 1.10$, $\log K_2 = \log K_9 = \log K_{14} = \log K_{15} = \log K_{21} = 0.80$, $\log K_3 = \log K_6 = \log K_{11} = \log K_{12} = \log K_{18} = 0.50$.

Table 4

Enthalpies of activation ($\Delta H^{\neq}$), entropies of activation ($\Delta S^{\neq}$) and free energies of activation at 25 °C ($\Delta G^{\neq}$) for the epoxidation of 3-methyl-2-buten-1-ol by aqueous H_2O_2 under biphasic conditions (1,2-dichloroethane/H_2O) using $[Ni_3(OH_2)_3(B\text{-}PW_9O_{34})\{WO_5(H_2O)\}]^{7-}$, $[Co_3(OH_2)_6(A\text{-}PW_9O_{34})_2]^{12-}$ and $[WZn\{Mn(OH_2)\}_2(B\text{-}ZnW_9O_{34})_2]^{12-}$ ions as catalysts.

Function	Rate constant	$[Ni_3(OH_2)_3(B\text{-}PW_9O_{34})\{WO_5(H_2O)\}]^{7-}$	$[Co_3(OH_2)_6(A\text{-}PW_9O_{34})_2]^{12-}$	$[WZn\{Mn(OH_2)\}_2(B\text{-}ZnW_9O_{34})_2]^{12-}$[a]
($\Delta H^{\neq}$) (kJ/mol)	k_4	5 (8)[b]	2 (14)	15 (5)
	k_5	38 (5)	42 (1)	50 (6)
	k_{10}	89 (4)	47 (5)	72 (3)
($\Delta S^{\neq}$) (J/K/mol)	k_4	−295 (24)	−304 (57)	−258 (15)
	k_5	−130 (15)	−111 (3)	−86 (20)
	k_{10}	49 (11)	−66 (19)	2 (9)
($\Delta G^{\neq}$) (kJ/mol)	k_4	93	93	92
	k_5	77	75	76
	k_{10}	74	67	71

[a] Data from [14]. (Note, k_4, k_5 and k_{10} in the current study correspond to k_3, k_4 and k_9, respectively, for a two-site system; see [14].)

[b] Standard deviations are given in parentheses and include fitting errors in the original rate constants.

previously studied $[WZn\{M(OH_2)\}_2(B\text{-}ZnW_9O_{34})_2]^{12-}$ series of ions, where M = Mn(II), Co(II), Ni(II), Cu(II) and Zn(II) for both series. The latter have been comprehensively studied as catalysts for the epoxidation of allylic alcohols under biphasic conditions [14], and this previous investigation formed the basis for the current studies. The two-site $[M_4(OH_2)_2(B\text{-}PW_9O_{34})_2]^{10-}$-type ions were therefore examined using identical reaction conditions (temperature, concentrations, etc.) to all of these previous studies to allow direct comparisons of catalytic activity.

Somewhat surprisingly, these anions were found to be much less active as epoxidation catalysts. Some comparative data on the epoxidation of the most reactive allylic alcohol used in this study, 3-methyl-2-buten-1-ol, is given in Table 5. Only the Cu(II)- and Ni(II)-substituted anions acted as oxygen transfer catalysts in these reactions at the temperature used in the studies (15 °C). It is apparent that from a comparison of the catalytic activity of the most active catalyst of this type, $[Cu_4(OH_2)_2(B\text{-}PW_9O_{34})_2]^{10-}$, with those of the three catalysts in Table 1 and the previously published data on the other four $[WZn\{M(OH_2)\}_2(B\text{-}ZnW_9O_{34})_2]^{12-}$ ions, where M = Co(II), Ni(II), Cu(II) and Zn(II) [14], that the $[M_4(OH_2)_2(B\text{-}PW_9O_{34})_2]^{10-}$ ions are the least active of all of these heteropolyoxotungstate anions. Indeed the most active $[M_4(OH_2)_2(B\text{-}PW_9O_{34})_2]^{10-}$ catalyst, that is $[Cu_4(OH_2)_2(B\text{-}PW_9O_{34})_2]^{10-}$, is less active than the least active of the five $[WZn\{M(OH_2)\}_2(B\text{-}ZnW_9O_{34})_2]^{12-}$ catalysts, that is $[WZn\{Ni(OH_2)\}_2(B\text{-}ZnW_9O_{34})_2]^{12-}$, under identical experimental conditions. Thus further studies of the $[M_4(OH_2)_2(B\text{-}PW_9O_{34})_2]^{10-}$ ions were not undertaken.

Unlike the $[WZn\{M(OH_2)\}_2(B\text{-}ZnW_9O_{34})_2]^{12-}$ series of ions, the catalytic activities of the $[M_4(OH_2)_2(B\text{-}PW_9O_{34})_2]^{10-}$ ions could not be related to the rate of exchange of the aqua groups on the M(II) ions in the waist of the sandwich anion [14]. However, the observed order of Cu(II) > Ni(II) > Zn(II) ~ Co(II) ~ Mn(II), although incomplete, is reminiscent of the Irving-Williams series or natural order of stability constants for the same first row (high-spin) transition metal ions, i.e. Mn(II) < Co(II) < Ni(II) < Cu(II) > Zn(II) [49]. Note that depending on the ligand, Zn(II) is to be found in a comparable position to Co(II) in this series.

The observed order suggests that catalytic activity in this series of anions is controlled by thermodynamic considerations, such as the magnitude of the equilibrium constant between the external aqua ligand and M(II). If this is large, then replacement of water by allylic alcohol will be much reduced (or cannot proceed) leading to this step in the mechanism being inaccessible so that no reaction will occur. Thus a stronger M–OH_2 linkage (a shorter bond) will lead to a reduced catalytic activity. This will obviously depend on temperature.

There are two lines of evidence that support this suggestion. The first comes from TG/DTA studies, which indicates the strength of retention of the two water molecules bound to the M(II) in the waist of the anions. The data have been presented previously in the Supplementary Material, Table S5, and the TG/DTA study for $K_{10}[Co_4(OH_2)_2(B\text{-}PW_9O_{34})_2]\cdot 20H_2O$ is shown in Fig. S3. The TG/DTA results show loss of both water of crystallization and constitutional (i.e. M(II)-coordinated) water and involves several steps, which at times overlap to a greater or lesser extent (see Fig. S3). For all five $[M_4(OH_2)_2(B\text{-}PW_9O_{34})_2]^{10-}$-containing compounds, where M = Mn(II), Co(II), Ni(II), Cu(II) and Zn(II), there are, in general, three identifiable stages from room temperature to the temperature of complete loss of water, although in the case of the $[Cu_4(OH_2)_2(B\text{-}PW_9O_{34})_2]^{10-}$ ion only two stages are observable. The highest temperature thermal step, based on the % of water lost can be assigned to loss of the two water molecules attached at the two M(II)-OH_2 sites in the waist of the anion, although there is some overlap with the second thermal stage, and complete overlap in the case of the Cu(II)-containing anion. Arranging the five $[M_4(OH_2)_2(B\text{-}PW_9O_{34})_2]^{10-}$ ions in the order of the temperature required for complete water loss from lowest to highest yields the order Ni(II) (198 °C) < Cu(II) (225 °C) < Co(II) (240 °C) < Mn(II) (250 °C) < Zn(II) (273 °C). It is noted that the two most catalytically active anions are also the ones that lose their constitutional water at the lowest temperatures. The actual order for the Ni(II)- and Cu(II)-containing anions (which is the reverse of their relative catalytic activities) may reflect the different cation compositions of these two compounds in the TG/DTA studies (K^+ vs Na^+/K^+). Of course, it should be recognized that TG/DTA is a dynamic

Table 5

Oxidation of 3-methyl-2-buten-1-ol by 30% aqueous H_2O_2 using the $[M_4(OH_2)_2(B\text{-}PW_9O_{34})_2]^{10-}$ ions, where M = Mn(II), Co(II), Ni(II), Cu(II) and Zn(II) in biphasic 1,2-dichloroethane/H_2O at 15 °C.[a]

Anion	% conversion	% H_2O_2 efficiency	TOF (h^{-1})	% aldehyde formation
$[Mn_4(OH_2)_2(B\text{-}PW_9O_{34})_2]^{10-}$	< 3	–	–	Not detected
$[Co_4(OH_2)_2(B\text{-}PW_9O_{34})_2]^{10-}$	< 3	–	–	Not detected
$[Ni_4(OH_2)_2(B\text{-}PW_9O_{34})_2]^{10-}$	14	79	47	Not detected
$[Cu_4(OH_2)_2(B\text{-}PW_9O_{34})_2]^{10-}$	41	70	135	Not detected
$[Zn_4(OH_2)_2(B\text{-}PW_9O_{34})_2]^{10-}$	< 3	–	–	Not detected

[a] Reaction conditions: Reactions were carried out at 15 °C for 3 h using 5 mmol of allylic alcohol, 2.5 mmol of *t*-butylbenzene (internal standard for gas chromatography), 5 µmol of catalyst, 20 µmol of Aliquat 336 and 10 mmol of H_2O_2.

experiment with a temperature ramp and also deals with solids as opposed to anions in solution. The same temperature ramp was used for all TG/DTA studies and the analyses were performed immediately following powdering of the solids, to minimize any differences in these studies. Nevertheless, the TG/DTA studies do suggest that water is not as easily removed from the Co(II), Mn(II) and Zn(II)-containing anions.

The second line of evidence comes from published crystallographic data on the five $[M_4(OH_2)_2(B\text{-}PW_9O_{34})_2]^{10-}$-containing compounds. Table 6 provides some structural data on the $[M_4(OH_2)_2(B\text{-}PW_9O_{34})_2]^{10-}$ ions, where M = Mn(II), Co(II), Ni(II), Cu(II) and Zn(II) (with the P^V replaced by As^V for the Zn(II) species), as well as on $[Fe_4^{III}(OH_2)_2(B\text{-}PW_9O_{34})_2]^{6-}$, the two $[WZn\{M(OH_2)\}_2(B\text{-}ZnW_9O_{34})_2]^{n-}$ ions, where M = Zn(II) and Rh(III), and $[WCu\{Cu(OH_2)\}_2(B\text{-}ZnW_9O_{34})_2]^{12-}$ for comparison [6,8,17,30,33–35]. Also included in Table 6 is the average M–OH_2 distance in the corresponding Tutton salts, $(NH_4)_2[M(OH_2)_6](SO_4)_2$, where M = Mn(II), Co(II), Ni(II), Cu(II) and Zn(II) (all have three crystallographically unique bonds, with standard deviations given in parentheses, except for the Jahn-Teller distorted bond in the Cu(II)-containing anion) [50], as well as the bond valences (BV) of the M(II)–OH_2 bonds in the heteropolyoxotungstate anions [51].

Although the errors in the crystallographic data are in some cases large, the results, with the exception of the Co(II)-containing polyoxotungstate anion are consistent with the observed catalytic activities; that is, bonds longer than expected are weaker, and thus will undergo H_2O-allylic alcohol exchange more readily, and vice versa. Note that all the 1st row transition metal M(II) ions (where M = Mn, Co, Ni, Cu and Zn) are normally labile. The Jahn-Teller distorted Cu-OH_2 bond is of course long (and hence weak), the Ni-OH_2 bond is normal in length, and the Mn-OH_2 and Zn-OH_2 bonds are short (and thus strong). The exception is the Co-OH_2 bond, which is long, but this has a large experimental error. It may be that a redetermination of the structure of this compound would show a much shorter bond than previously reported. We note that in the original crystallographic paper Evans et al. did report that the H_2O ligands in $[Co_4(OH_2)_2(B\text{-}PW_9O_{34})_2]^{10-}$ could not be replaced with strong donors, such as pyridine and anions such as SCN^- [33]. However, Zhang et al. have reported that in acetonitrile solution the water ligands in $[Co_4(OH_2)_2(B\text{-}PW_9O_{34})_2]^{10-}$ can be replaced by strong donors such as *N*-methylimidazole, and the three *N*-oxides, 4-picoline *N*-oxide, 4-cyanopyridine *N*-oxide and *N*-methylmorpholine *N*-oxide [47]. Note that the bond valences (defined as cation charge/coordination) for the five M^{II}-(OH_2) bonds of the $[M_4(OH_2)_2(B\text{-}PW_9O_{34})_2]^{10-}$ series of ions (Table 6), which is $+2/6 = 0.33$ for a standard M(II)–OH_2 bond in an $[M(OH_2)_6]^{2+}$ ion, show that the bonds are very strong for Zn(II) and Mn(II) (both with BV > 0.33), about as expected for Ni(II) (BV ~ 0.33) and quite weak for Cu(II) (BV < 0.33). This parallels the catalytic activities as discussed above. The BV value for the Zn(II)–OH_2 bond in $[WZn\{Zn(OH_2)\}_2(B\text{-}ZnW_9O_{34})_2]^{12-}$ indicates a weak bond, which is consistent with its known catalytic activity [14]. The BV value for the Co(II)–OH_2 bond in $[Co_4(OH_2)_2(B\text{-}PW_9O_{34})_2]^{10-}$ is weaker than expected (BV < 0.33), and not in agreement with the observed catalytic activity, as noted above.

The one question that remains to be answered is why is it that the $[M_4(OH_2)_2(B\text{-}PW_9O_{34})_2]^{10-}$ series of anions is much less reactive than the $[WZn\{M(OH_2)\}_2(B\text{-}ZnW_9O_{34})_2]^{12-}$ series of anions, where M = Mn(II), Co(II), Ni(II), Cu(II) and Zn(II) in both series? The major difference between the two series is that the Zn(II) in the $[B\text{-}ZnW_9O_{34}]^{12-}$ ion has been replaced by P(V) in the $[B\text{-}PW_9O_{34}]^{9-}$ ion. The P(V) has a much smaller tetracoordinated ionic radius than Zn(II), with Zn(II) = 0.74 Å and P(V) = 0.31 Å (note As(V) = 0.59 Å) [52], so that a P—O bond (about 1.53 Å) is much shorter than a Zn-O bond (1.96 Å). This difference has an effect on the length of the M – O bond that is *trans* to the externally directed M – OH_2 bond. The oxygen atom of the M – O bond *trans* to the M – OH_2 bond is attached to the centrally located P (or As) and Zn atom of the $[B\text{-}P(\text{or As})W_9O_{34}]^{9-}$ and $[B\text{-}ZnW_9O_{34}]^{12-}$ ions. However, the crystallographic data show that the P (or As) atoms are all about the same distance from the center of inversion in these anions, which is located in the plane of the four metal atoms in the waist of the structures (2.81–2.94 Å). Likewise, in the $[WZn\{M(OH_2)\}_2(B\text{-}ZnW_9O_{34})_2]^{12-}$ series of anions the Zn is about the same distance from the center of inversion (2.91–2.94 Å). This means that the distance from the M(II) to the oxygen atom *trans* to the coordinated H_2O, i.e. M – O(Z), where Z = P, As or Zn, will be necessarily longer in the $[M_4(OH_2)_2(B\text{-}PW_9O_{34})_2]^{10-}$ series of anions compared to those in the $[WZn\{M(OH_2)\}_2(B\text{-}ZnW_9O_{34})_2]^{12-}$ series. In order to maintain the bond valence sum around the M(II) atoms, the M – OH_2 distance is thus affected, by shortening, thereby making it more difficult to lose coordinated water and replace it by an allylic alcohol. The effect of changing the Zn(II) to a P(V) or As(V) is better seen by comparing the {M–O(Z)} – {M–OH_2} distance in the anions. In the $[M_4(OH_2)_2(B\text{-}PW_9O_{34})_2]^{10-}$ series of anions this value is positive, while in the $[WZn\{M(OH_2)\}_2(B\text{-}ZnW_9O_{34})_2]^{12-}$ and related series of anions (Table 6) this value is negative, showing the lengthening of the bond *trans* to M in the $[M_4(OH_2)_2(B\text{-}PW_9O_{34})_2]^{10-}$ series of anions and reduction in the length of the M – OH_2 bond. This results in a reduction in catalytic activity for the $[M_4(OH_2)_2(B\text{-}PW_9O_{34})_2]^{10-}$ series of anions. Finally, IR studies of the type performed on $[Ni_3(OH_2)_3(B\text{-}PW_9O_{34})\{WO_5(H_2O)\}]^{7-}$, as described above, showed that $W(O_2)$ formation easily occurred for $[Ni_4(OH_2)_2(B\text{-}PW_9O_{34})_2]^{10-}$ and $[Zn_4(OH_2)_2(B\text{-}PW_9O_{34})_2]^{10-}$ with bands at 827 and 826 cm^{-1}, respectively. The former acts as a catalyst under the reaction conditions (Table 5), while the latter does not. Thus peroxo formation is

Table 6

Relevant structural data concerning the M – OH_2 bonds in the $[M_4(OH_2)_2(B\text{-}PW_9O_{34})_2]^{10-}$ ions, where M = Mn(II), Co(II), Ni(II), Cu(II) and Zn(II) (for the last P^V is replaced by As^V), $[Fe_4^{III}(OH_2)_2(B\text{-}PW_9O_{34})_2]^{6-}$, the $[WZn\{M(OH_2)\}_2(B\text{-}ZnW_9O_{34})_2]^{n-}$ ions, where M = Zn(II) and Rh(III), and $[WCu\{Cu(OH_2)\}_2(B\text{-}ZnW_9O_{34})_2]^{12-}$, together with data on the M – OH_2 distances in the Tutton salts, $(NH_4)_2[M(OH_2)_6](SO_4)_2$, and bond valences (BV) of the M – OH_2 bonds in the heteropolyoxotungstate anions.

Anion	M – OH_2 (Å)	M – O(Z) (Å)[a]	Diff. (Å)[b]	Av. M^{II}-OH_2 for T.S. (Å)[c]	BV of M^{II}-OH_2 bond
$[Mn_4(OH_2)_2(PW_9O_{34})_2]^{10-}$	2.15(2)	2.27(1)	0.12	2.18(2)	0.38
$[Co_4(OH_2)_2(PW_9O_{34})_2]^{10-}$	2.15(4)	2.17(3)	0.02	2.09(2)	0.29
$[Ni_4(OH_2)_2(PW_9O_{34})_2]^{10-}$	2.05(2)	2.14(2)	0.09	2.06(1)	0.34
$[Cu_4(OH_2)_2(PW_9O_{34})_2]^{10-}$	2.34(2)	2.55(1)	0.21	2.222(1)[d]	0.17
$[Zn_4(OH_2)_2(AsW_9O_{34})_2]^{10-}$	2.04(3)	2.18(2)	0.14	2.09(2)	0.40
$[Fe_4^{III}(OH_2)_2(PW_9O_{34})_2]^{6-}$	2.002(9)	2.169(2)	0.17	–	–
$[WZn\{Zn(OH_2)\}_2(ZnW_9O_{34})_2]^{12-}$	2.17(2)	2.07(2)	−0.10	–	0.28
$[WZn\{Rh^{III}(OH_2)\}_2(ZnW_9O_{34})_2]^{10-}$	2.14[e]	2.09[e]	−0.05	–	–
$[WCu\{Cu(OH_2)\}_2(ZnW_9O_{34})_2]^{12-}$	2.08(2)	2.00(2)	−0.08	–	0.34

[a] Z is the heteroatom in the $[ZW_9O_{34}]^{n-}$ anion, i.e. P(V), As(V) or Zn(II).

[b] Diff. = {M – O(Z)} – {M – OH_2} distance. These two bonds are *trans* to each other.

[c] T.S. is the equivalent Tutton salt, $(NH_4)_2[M(OH_2)_6](SO_4)_2$. The data are taken from [50].

[d] Long M – OH_2 bond in Jahn-Teller-distorted structure rather than the average M – OH_2 bond, which is 2.09(11) Å for the Cu(II)-containing Tutton salt.

[e] No standard deviations provided in original manuscript [8].

not an impediment to the reaction mechanism in this case, with allylic alcohol coordination to M(II) the actual determining step in the reaction.

4. Conclusions

The epoxidation of a range of allylic alcohols using the three-site $[Ni_3(OH_2)_3(B\text{-}PW_9O_{34})\{WO_5(H_2O)\}]^{7-}$ and $[Co_3(OH_2)_6(A\text{-}PW_9O_{34})_2]^{12-}$ ions as catalysts with aqueous H_2O_2 as the oxidant has been studied and compared with previous data on the $[WZn\{Mn(OH_2)\}_2(B\text{-}ZnW_9O_{34})_2]^{12-}$ ion. The Co_3-containing anion proved to be a more active catalyst under identical reaction conditions, while the Ni_3-containing anion was less active than the two-site system. Both the Ni_3- and Co_3-containing anions operate by an identical reaction mechanism to that previously established for $[WZn\{Mn(OH_2)\}_2(B\text{-}ZnW_9O_{34})_2]^{12-}$, except with three active M(II) sites rather than two M(II) sites. Kinetic studies of the epoxidation of 3-methyl-2-buten-1-ol by aqueous H_2O_2 showed the presence of induction steps which could be interpreted in terms of an autocatalysis mechanism. The mechanism involves coordination of an allylic alcohol to a M(II), along with formation of an adjacent $W(O_2)$ from a W═O. Subsequent transfer of the O from the $W(O_2)$ to the allylic alcohol generates the hydroxy epoxide. The mechanism involves some twenty-one steps for the three M(II) sites, with the autocatalysis arising because coordination of the product hydroxy epoxide competes with coordination of the allylic alcohol and must be replaced by the latter for reaction to occur, while $W(O_2)$ formation occurs much more readily when the M(II) is coordinated by hydroxy epoxide than by allylic alcohol.

Studies of the related $[M_4(OH_2)_2(B\text{-}PW_9O_{34})_2]^{10-}$ series of anions, where M = Mn(II), Co(II), Ni(II), Cu(II) and Zn(II), indicates that all are much less catalytically active than the $[WZn\{M(OH_2)\}_2(B\text{-}ZnW_9O_{34})_2]^{12-}$ series of anions, and this is attributed to the replacement of $[B\text{-}ZnW_9O_{34}]^{12-}$ by $[B\text{-}PW_9O_{34}]^{9-}$, and more specifically as the replacement of Zn(II) by P(V) affects the adjoining $M-O(Z)$ distance, which in turn affects the (externally directed) *trans* $M-OH_2$ distance by shortening, making these anions less catalytically active. This, of course, assumes that an identical reaction mechanism also operates for these $[M_4(OH_2)_2(B\text{-}PW_9O_{34})_2]^{10-}$ series of anions, which is most likely.

Declaration of Competing Interest

The authors declare that they have no known competing financial interests or personal relationships that could have appeared to influence the work reported in this paper.

Acknowledgments

P. H. A. would like to acknowledge a scholarship and financial support from the Ministry of Research, Technology and Higher Education, Indonesia (DIKTI-Scholarship), as well as a UNRS and OPRS from the University of Newcastle. Prof. M. Maeder is thanked for access to the ReactLab programs.

This research did not receive any specific grant from funding agencies in the public, commercial, or not-for-profit sectors.

Appendix A. Supplementary data

Supplementary data to this article can be found online at https://doi.org/10.1016/j.ica.2019.119178.

References

[1] C.L. Hill, Comprehensive Coordination Chemistry II: From Biology to Nanotechnology, Elsevier, Oxford, 2004, pp. 679–759.
[2] R. Neumann, Transition Metals for Organic Synthesis, second ed., Wiley-VCH, Weinheim, 2004, pp. 415–426.
[3] I.V. Kozhevnikov (Ed.), Catalysis by Polyoxometalates, Wiley, Chichester, England, 2002Vol. 2.
[4] N. Mizuno, M. Misono, Chem. Rev. 98 (1998) 199–218.
[5] C.L. Hill, C.M. Prosser-McCartha, Coordination Chem. Rev. 143 (1995) 407–455.
[6] C.M. Tourné, G.F. Tourné, F. Zonnevijlle, J. Chem. Soc., Dalton Trans. (1991) 143–155.
[7] R. Neumann, A.M. Khenkin, Inorg. Chem. 34 (1995) 5753–5760.
[8] R. Neumann, A.M. Khenkin, J. Mol. Catal. A: Chem. 114 (1996) 169–180.
[9] R. Neumann, M. Gara, J. Am. Chem. Soc. 116 (1994) 5509–5510.
[10] R. Neumann, M. Gara, J. Am. Chem. Soc. 117 (1995) 5066–5074.
[11] W. Adam, P.L. Alsters, R. Neumann, C.R. Saha-Möller, D. Sloboda-Rozner, R. Zhang, J. Org. Chem. 68 (2003) 1721–1728.
[12] R. Neumann, D. Juwiler, Tetrahedron 52 (1996) 8781–8788.
[13] R. Neumann, A.M. Khenkin, D. Juwiler, H. Miller, M. Gara, J. Mol. Catal. A: Chem. 117 (1997) 169–183.
[14] R.C. Burns, P.H. Abram, Trans. Metal Chem. 43 (2018) 705–717.
[15] A.J. Stapleton, M.E. Sloan, N.J. Napper, R.C. Burns, Dalton Trans. 38 (2009) 9603–9615.
[16] R. Ben-Daniel, A.M. Khenkin, R. Neumann, Chem. Eur. J. 6 (2000) 3722–3728.
[17] X. Zhang, Q. Chen, D.C. Duncan, R.J. Lachicotte, C.L. Hill, Inorg. Chem. 36 (1997) 4381–4386.
[18] X. Zhang, Q. Chen, D.C. Duncan, C.F. Campana, C.L. Hill, Inorg. Chem. 36 (1997) 4208–4215.
[19] A.M. Khenkin, C.L. Hill, Mendeleev Commun. (1993) 140–141.
[20] M. Bösing, A. Nöh, I. Loose, B. Krebs, J. Am. Chem. Soc. 120 (1998) 7252–7259.
[21] K.A. Jørgensen, Chem. Rev. 89 (1989) 431–458.
[22] W. Adam, T. Wirth, Acc. Chem. Res. 32 (1999) 703–710.
[23] P.A. Bartlett, Tetrahedron 36 (1980) 2–72.
[24] P. Besse, H. Veschambre, Tetrahedron 50 (1994) 8885–8927.
[25] D. Sloboda-Rozner, R. Neumann, Green Chem. 8 (2006) 679–681.
[26] Y. Qiao, Z. Hou, Curr. Org. Chem. 13 (2009) 1347–1365.
[27] S. Omwoma, C.T. Gore, Y. Ji, C. Hu, Coord. Chem. Rev. 286 (2015) 17–29.
[28] S.-Y. Dou, R. Wang, Curr. Org. Chem. 21 (2017) 1019–1036.
[29] C.J. Gómez-Garcia, E. Coronado, L. Ouahab, Angew. Chem. Int. Ed. Engl. 31 (1992) 649–651.
[30] J.M. Clemente-Juan, E. Coronado, J.R. Galán-Mascarós, C.J. Gómez-Garcia, Inorg. Chem. 38 (1999) 55–63.
[31] W.H. Knoth, P.J. Domaille, R.D. Farlee, Organometallics 4 (1985) 62–68.
[32] T.J.R. Weakley, H.T. Evans Jr, J.S. Showell, G.F. Tourné, C.M. Tourné, J. Chem. Soc., Chem. Commun. (1973) 139–140.
[33] H.T. Evans, C.M. Tourné, G.F. Tourné, T.J.R. Weakley, J. Chem. Soc., Dalton Trans. (1986) 2699–2705.
[34] C.J. Gómez-Garcia, E. Coronado, P. Gómez-Romero, N. Casañ-Pastor, Inorg. Chem. 32 (1993) 3378–3381.
[35] T.J.R. Weakley, R.G. Finke, Inorg. Chem. 29 (1990) 1235–1241.
[36] R.G. Finke, M. Droege, J.R. Hutchinson, O. Gansow, J. Am. Chem. Soc. 103 (1981) 1587–1589.
[37] R.D. Mair, R.T. Hall, in: I.M. Kolthoff, P.J. Elving (Eds.) Treatise on Analytical Chemistry. Part II. Analytical Chemistry of Inorganic and Organic Compounds, Wiley-Interscience, 1971, Vol. 14, p 411.
[38] http://www.jplusconsulting.com/products.
[39] R. Massart, R. Contant, J.M. Fruchart, J.P. Ciabrini, M. Fournier, Inorg. Chem. 16 (1977) 2916–2921.
[40] R.G. Finke, M.W. Droege, P.M. Domaille, Inorg. Chem. 26 (1987) 3886–3896.
[41] W.H. Knoth, P.J. Domaille, R.L. Harlow, Inorg. Chem. 25 (1986) 1577–1584.
[42] P.H. Abram, Ph. D. Thesis, The University of Newcastle, NSW, Australia, 2014.
[43] C. Dean, R. Duncan, C. Chambers, E. Hecht, C.L. Hill, J. Am. Chem. Soc. 117 (1995) 681–691.
[44] R.B. Jordan, Reaction Mechanisms of Inorganic and Organometallic Systems, Oxford University Press, New York, 1991.
[45] P.C. Harris, T.E. Moore, Inorg. Chem. 7 (1968) 656–660.
[46] R.F. Pasternack, R.A. Plane, Inorg. Chem. 4 (1965) 1171–1173.
[47] X. Zhang, K. Sasaki, C.L. Hill, J. Am. Chem. Soc. 118 (1996) 4809–4816.
[48] IUPAC Stability Constants Database, Academic Software, 2006. See the section on the "K v T Temp. Dependence", under "Definitions".
[49] C.E. Housecroft, A.G. Sharpe, Inorganic Chemistry, fourth ed., Pearson Education Ltd, England, 2012 Sec. 20.12, pp 709-710.
[50] F.A. Cotton, L.M. Daniels, C.A. Murillo, J.F. Quesada, Inorg. Chem. 32 (1993) 4861–4867.
[51] I.D. Brown, D. Altermatt, Acta Crystallogr. B 41 (1985) 244–247.
[52] R.D. Shannon, Acta Crystallogr. A 32 (1976) 751–767.